Spectrin mutations that cause spinocerebellar ataxia type 5 impair axonal transport and induce neurodegeneration in *Drosophila*

Damaris N. Lorenzo,[1,2] Min-gang Li,[2] Sarah E. Mische,[2] Karen R. Armbrust,[1,2] Laura P. W. Ranum,[1,2] and Thomas S. Hays[2]

[1]Institute of Human Genetics and [2]Department of Genetics, Cell Biology, and Development, University of Minnesota, Minneapolis, MN 55455

Spinocerebellar ataxia type 5 (SCA5) is an autosomal dominant neurodegenerative disorder caused by mutations in the *SPBTN2* gene encoding β-III–spectrin. To investigate the molecular basis of SCA5, we established a series of transgenic *Drosophila* models that express human β-III–spectrin or fly β-spectrin proteins containing SCA5 mutations. Expression of the SCA5 mutant spectrin in the eye causes a progressive neurodegenerative phenotype, and expression in larval neurons results in posterior paralysis, reduced synaptic terminal growth, and axonal transport deficits. These phenotypes are genetically enhanced by both dynein and dynactin loss-of-function mutations. In summary, we demonstrate that SCA5 mutant spectrin causes adult-onset neurodegeneration in the fly eye and disrupts fundamental intracellular transport processes that are likely to contribute to this progressive neurodegenerative disease.

Introduction

Spinocerebellar ataxia type 5 (SCA5) is an autosomal dominant neurodegenerative disease that primarily affects the cerebellum. Affected patients have progressive cerebellar cortical atrophy and profound Purkinje cell loss. Similar clinical presentations reported in three different SCA5 families include upper and lower limb incoordination, slurred speech, and eye movement abnormalities. Age of onset typically occurs during the third or fourth decade of life, and symptoms worsen over time (Liquori et al., 2002). SCA5 is caused by mutations in the *SPTBN2* gene, which encodes β-III–spectrin, a cytoskeletal protein highly expressed in Purkinje cells (Ikeda et al., 2006). An American and a French SCA5 family have distinct, nonoverlapping in-frame deletions in the third of the 17 spectrin repeats, and both of these deletions are predicted to disrupt the triple α-helical structure of the spectrin repeat and the conformation of the spectrin tetramer. A third reported SCA5 family, from Germany, has a missense mutation in the second calponin homology domain. This region of the protein has been reported to bind actin and the ARP1 subunit of dynactin, providing a link between the actin cytoskeletal network and motor proteins (Holleran et al., 2001).

Although it is not yet clear how β-III–spectrin mutations cause Purkinje cell death in SCA5 patients, several lines of evidence have led to the proposal that SCA5 pathogenesis could result from the destabilization of specialized synaptic membrane domains and/or defects in intracellular transport. First, wild-type but not mutant β-III–spectrin stabilizes the Purkinje cell–specific excitatory amino acid transporter 4 (EAAT4) at the surface of the plasma membrane (Ikeda et al., 2006). In addition, cell fractionation studies have shown differences in the localization of EAAT4 and the glutamate receptor delta 2 subunit (GluRδ2) in cerebellar synaptosomal fractions from SCA5 versus control autopsy tissue (Ikeda et al., 2006), and the C-terminal domains of GluRδ2 and EAAT4 have been shown to physically interact with spectrin (Hirai and Matsuda, 1999; Jackson et al., 2001). Finally, β-III–spectrin is a Golgi- and vesicle-associated protein that interacts with dynactin (Holleran et al., 2001). This

Correspondence to Laura P.W. Ranum: ranum001@umn.edu; or Thomas S. Hays: haysx001@umn.edu

Abbreviations used in this paper: CSP, cysteine string protein; EAAT4, excitatory amino acid transporter 4; Fas II, fasciclin II; FSPAM, fly spectrin American mutant; FSPGM, fly spectrin German mutant; FSPWT, fly spectrin wild type; hSPAM, human spectrin American mutation; hSPGM, human spectrin German mutation; hSPWT, human spectrin wild type; NMJ, neuromuscular junction; n-syb, neuronal synaptobrevin; RIPA, radio immunoprecipitation assay; SCA5, spinocerebellar ataxia type 5; syt, synaptotagmin.

The Rockefeller University Press $30.00
J. Cell Biol. Vol. 189 No. 1 143–158
www.jcb.org/cgi/doi/10.1083/jcb.200905158

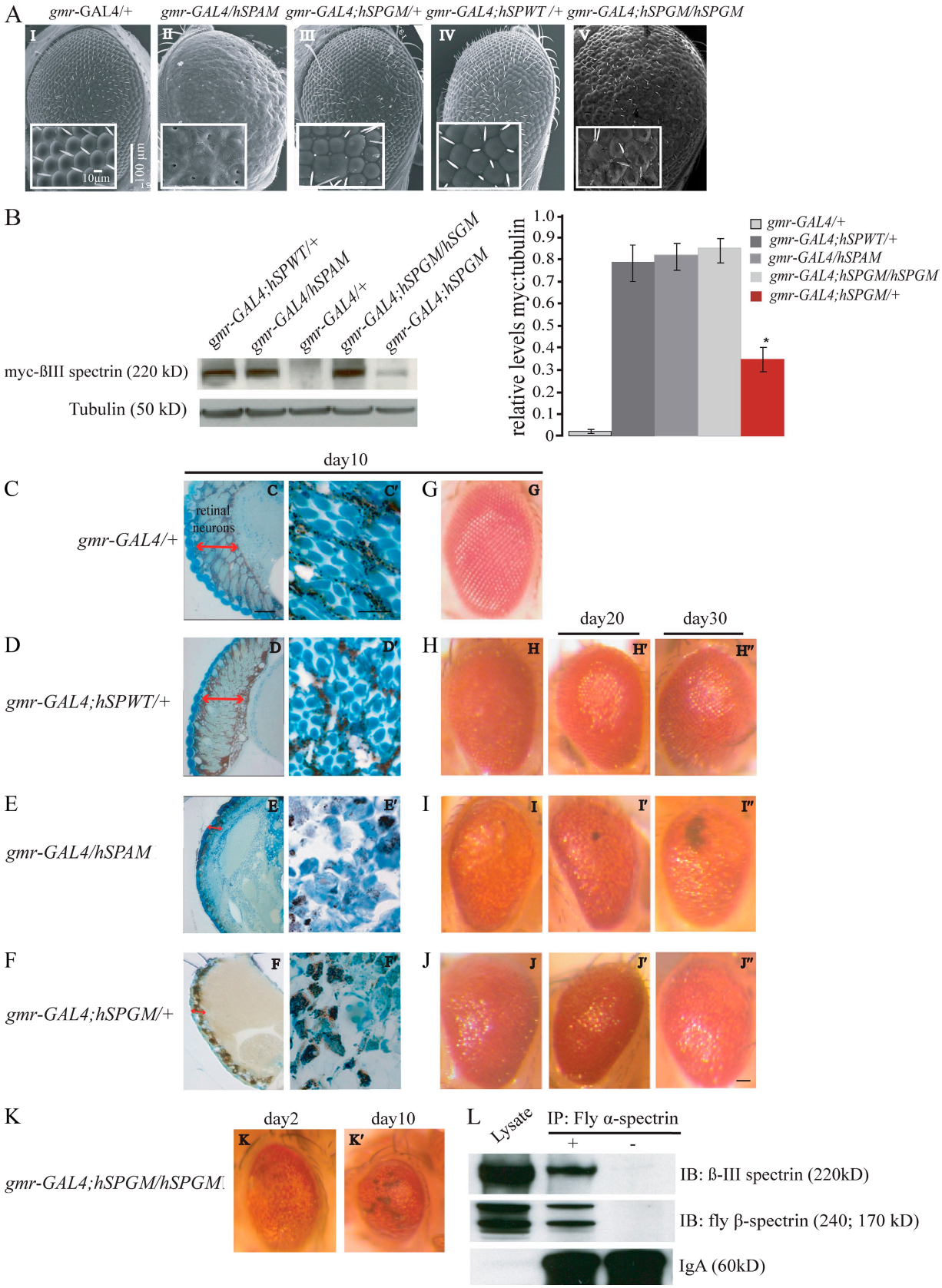

Figure 1. **Expression of mutant β-III–spectrin causes a dosage-dependent and progressive neurodegenerative eye phenotype.** (A) Scanning EM images of adult fly eyes grown at 25°C. Insets show higher magnification images of ommatidial fields. Expression of the American SCA5 mutation in human β-III–spectrin in the eye results in a fused and disorganized ommatidia missing interommatidial bristles (II). Flies expressing the German SCA5 mutation in β-III–spectrin show a mild roughness of the eye (III), with a more severe phenotype in flies expressing two copies of the German SCA5 transgene (V). Flies expressing wild-type β-III–spectrin show only a mild ommatidial phenotype similar to *gmr-GAL4* control flies (I and IV). Similar disruption of ommatidial

interaction is thought to be required for proper cargo attachment and motor activity (Muresan et al., 2001). Although data from in vitro biochemical experiments support a role for β-III–spectrin in intracellular transport, in vivo models are needed to test if SCA5 mutations cause neuronal transport deficits.

Because *Drosophila* has proven to be an excellent organism to model basic cellular defects of human neurodegenerative disease (for review see Bilen and Bonini, 2005), we have developed a *Drosophila* model to investigate the molecular mechanisms of SCA5. The fly genome contains one α-spectrin, one conventional β-spectrin, and one heavy spectrin (β_H-spectrin) gene, each of which is highly expressed at both central and peripheral synapses. Fly β-spectrin shares 50% amino acid homology with human β-III–spectrin, as well as conservation of all functional domains, including each of the regions containing the human mutations (Fig. S1 A, I and II).

Similar to human β-III–spectrin, fly β-spectrin has also been implicated in membrane stabilization and intracellular transport functions. Loss or reduced expression of fly β-spectrin in neurons results in severe defects in the formation and stabilization of synaptic junctions (Pielage et al., 2005, 2006). Segmental axons from larvae in which expression of β-spectrin has been ubiquitously abolished or conditionally eliminated in neurons show aberrant distribution of synaptic proteins, which accumulate within axonal swellings (Featherstone et al., 2001; Pielage et al., 2005, 2006).

Here, we show that expression of SCA5 mutant, but not wild-type, β-spectrin proteins causes neurodegeneration in the fly eye and deficits in synapse formation at the neuromuscular junction (NMJ). Additionally, we present live imaging and genetic evidence that the SCA5 mutations disrupt intracellular transport, a basic cell biological process also implicated in several other neurodegenerative diseases including amyotrophic lateral sclerosis and Huntington's disease (De Vos et al., 2008).

Results

Expression of human SCA5 mutant β-III–spectrins cause dosage-dependent, progressive neurodegeneration in the *Drosophila* eye

To understand the molecular mechanisms of SCA5, we cloned the full-length myc-tagged human *SPTBN2* cDNA carrying the wild-type sequence (human spectrin wild type [*hSPWT*]), mutations found in an American family descended from President Abraham Lincoln's paternal grandparents (human spectrin American mutation [*hSPAM*]; Ikeda et al., 2006), or a German family (human spectrin German mutation [*hSPGM*]; Ikeda et al., 2006) into the transformation vector *pUASp* (Fig. S1 B) and performed embryo injections. The resulting transgenic flies were crossed to the eye-specific *gmr-GAL4* driver (Freeman, 1996) to ectopically express the human transgenes in the eye. Expression of human β-III–spectrin with the American family mutation (*gmr-GAL4/hSPAM*) results in a severe rough eye phenotype characterized by disorganized ommatidia and loss of mechanosensory bristles (Fig. 1 A, II), whereas expression of the German mutant spectrin (*gmr-GAL4/+; hSPGM/+*) causes a milder eye phenotype (Fig. 1 A, III). In contrast, expression of wild-type human β-III–spectrin (*gmr-GAL4/+; hSPWT/+*) causes only a very mild ommatidial phenotype that does not disrupt normal eye development (Fig. 1 A, IV) and is similar to the control driver flies (*gmr-GAL4/+*; Fig. 1 A, I). Protein analysis shows that flies expressing wild-type (*gmr-GAL4/+; hSPWT/+*) and the American mutant spectrin (*gmr-GAL4/hSPAM*) produce comparable levels of transgenic protein, whereas flies expressing the German mutant spectrin (*gmr-GAL4/+; hSPGM/+*) have significantly lower β-III–spectrin expression (Fig. 1 B; $P = 0.025$, $n = 4$). As expected the phenotypes are dosage dependent; flies carrying two copies of the *hSPGM* transgene (*gmr-GAL4/+; hSPGM/hSPGM*) express higher levels of β-III–spectrin compared with the heterozygous flies (Fig. 1 B) and develop a stronger rough eye phenotype (Fig. 1 A, V).

To determine if the SCA5 spectrin mutations affect retinal neurons, histological analysis was performed. Sections taken through the eye of 10-d-old flies showed a severe disruption of the retinal organization, with thinning of the retina and loss of retinal neurons in flies expressing the American and German SCA5 mutations (Fig. 1, E, E′, F, and F′, see arrows) compared with the *gmr-GAL4* driver line (Fig. 1, C and C′) or flies expressing wild-type β-III–spectrin (Fig. 1, D and D′). Analysis of flies expressing the SCA5 mutations revealed that the extent of neurodegeneration in the eye became more severe as flies aged. By day 30, eyes from flies expressing the American SCA5 mutation showed dramatic changes in pigmentation and abundant necrotic tissue (Fig. 1, I–I″). Similarly, heterozygous flies

organization was observed when the mutant, but not wild-type, spectrin transgenes were expressed using the neuronal-specific *nina E-GAL4* driver. (B, right) Bar graph showing mean ratios of myc-tagged spectrin versus tubulin protein for control *gmr-GAL4/+*, *gmr-GAL4/+; hSPWT/+*, *gmr-GAL4/hSPAM; gmr-GAL4/+; hSPGM/+*, and homozygous *gmr-GAL4/+; hSPGM/hSPGM* flies. Animals expressing one copy of the hSPGM transgene have a significant reduction in β-III–spectrin expression ($P = 0.025$, $n = 4$). Data represent mean ± SEM; *, $P = 0.025$. (B, left) β-III–spectrin expression for the different genotypes was detected using an antibody to the myc epitope with tubulin as a loading control. (C–F) Histological sections of fly eyes. Longitudinal frontal sections (C–F) and tangential sections (panels C′–F′) taken through the retina of 10-d-old flies. Images show thinning of the retinal layer (arrow) and loss of retinal neurons (arrowhead) in flies expressing the American (E and E′) and German (F and F′) SCA5 mutations compared with a wild-type control (D and D′) and *gmr-GAL4* driver flies (C and C′). (G–J″) Optical eye images taken at days 10, 20, and 30 illustrate the progression of the eye phenotype. Flies expressing wild-type human β-III–spectrin had external eye morphology similar to the *gmr-GAL4* driver (G), and showed no changes in ommatidia organization and pigmentation during the first 30 d of adult life (H–H″). The eye phenotype of flies expressing the American mutant spectrin worsens considerably over time (I–I″). Flies expressing low levels of the German mutant spectrin have defects in pigmentation by day 30 (J″). (K and K′) Optical eye images taken at days 2 and 10 correspond to flies expressing two copies of the *hSPGM* transgene. The severity and progression of the rough eye phenotype worsens with increasing dosage of mutant German β-III–spectrin. (L) Protein extracts from flies expressing the wild-type human β-III–spectrin transgene (*gmr-GAL4/+; hSPWT/+*) were subjected to immunoprecipitation using the anti–fly α-spectrin monoclonal antibody 3A9. Precipitated immune complexes were then analyzed by Western blotting assays using either anti-myc or anti-fly β-spectrin antibodies. BSA was used as a control for the immunoprecipitation reaction. Bars: (C–F) 50 μm; (C′–F′): 5 μm; (G–K) 50 μm.

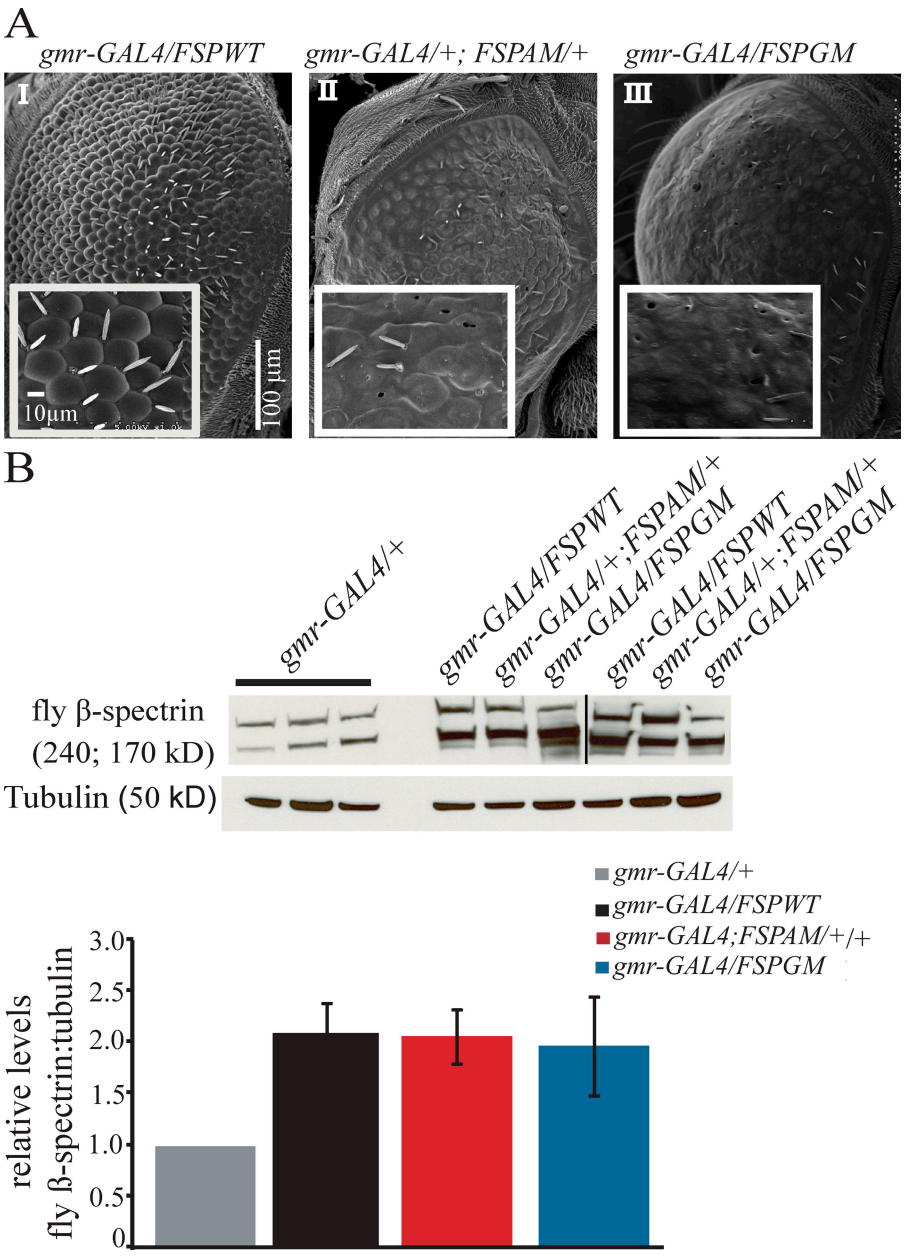

Figure 2. **Human β-III–spectrin and fly β-spectrin share functional pathways.** (A) Scanning EM images of adult eyes from flies grown at 25°C. Insets show higher magnification images of the ommatidia field. Expression of fly β-spectrin carrying either the American (*gmr-GAL4/+; FSPAM/+, II*) or German (*gmr-GAL4/FSPGM, III*) SCA5 mutations in the adult fly eye results in a neurodegenerative eye phenotype. Overexpressing wild-type fly β-spectrin (*gmr-GAL4/FSPWT, I*) results in minor changes in the external morphology of the eye similar to the *gmr-GAL4* control. (B, top) Total proteins from fly heads were analyzed by Western blotting using an antibody that recognizes fly β-spectrin. Tubulin was used as a loading control. The black line indicates that intervening lanes have been spliced out. (B, bottom) Bar graphs showing mean ratios of fly β-spectrin versus tubulin protein. The expression of fly β-spectrin in each transgenic line was similar and approximately twice the endogenous level of protein detected in the *gmr*-GAL4/+ driver line ($P = 0.18$, $n = 4$). Error bars indicate mean ± SEM (error bars); *, $P = 0.18$.

expressing low levels of the German SCA5 mutation developed eye pigmentation abnormalities by day 30 (Fig. 1, J–J″), whereas homozygous flies expressing higher levels of German mutant spectrin showed dramatic changes in eye pigmentation by day two, and patches of severe necrosis by day 10 (Fig. 1, K and K′). In contrast, no changes in external eye morphology or pigmentation were found in control flies expressing wild-type β-III–spectrin (Fig. 1, H and H″). Taken together, these results demonstrate that expression of human β-III–spectrin containing either the American or German mutations causes a progressive, dominant neurodegenerative phenotype.

The basic structural unit of the spectrin network is a dimer formed by direct association between α- and β-spectrin subunits (for review see Bennett and Baines, 2001). To begin to understand the molecular basis for the observed neurodegenerative phenotypes, we tested whether human β-III–spectrin assembles into the fly α/β-spectrin complex by immunoprecipitation (Fig. 1 L). Proteins from flies expressing wild-type human β-III–spectrin in the eye were immunoprecipitated with anti-fly α-spectrin antibody, and protein blot analysis shows that human β-III–spectrin and fly α-spectrin interact. This result indicates that the human β-III–spectrin does appear to incorporate into the α/β-spectrin complexes in flies.

Human β-III–spectrin and fly β-spectrin share some binding partners and functional pathways

To further characterize the effects of the SCA5 mutations, we developed a second set of transgenic flies in which the human SCA5 mutations were incorporated into *Drosophila* cDNA constructs designed to overexpress wild-type (fly spectrin wild type [*FSPWT*]) and mutant fly β-spectrins (fly spectrin American

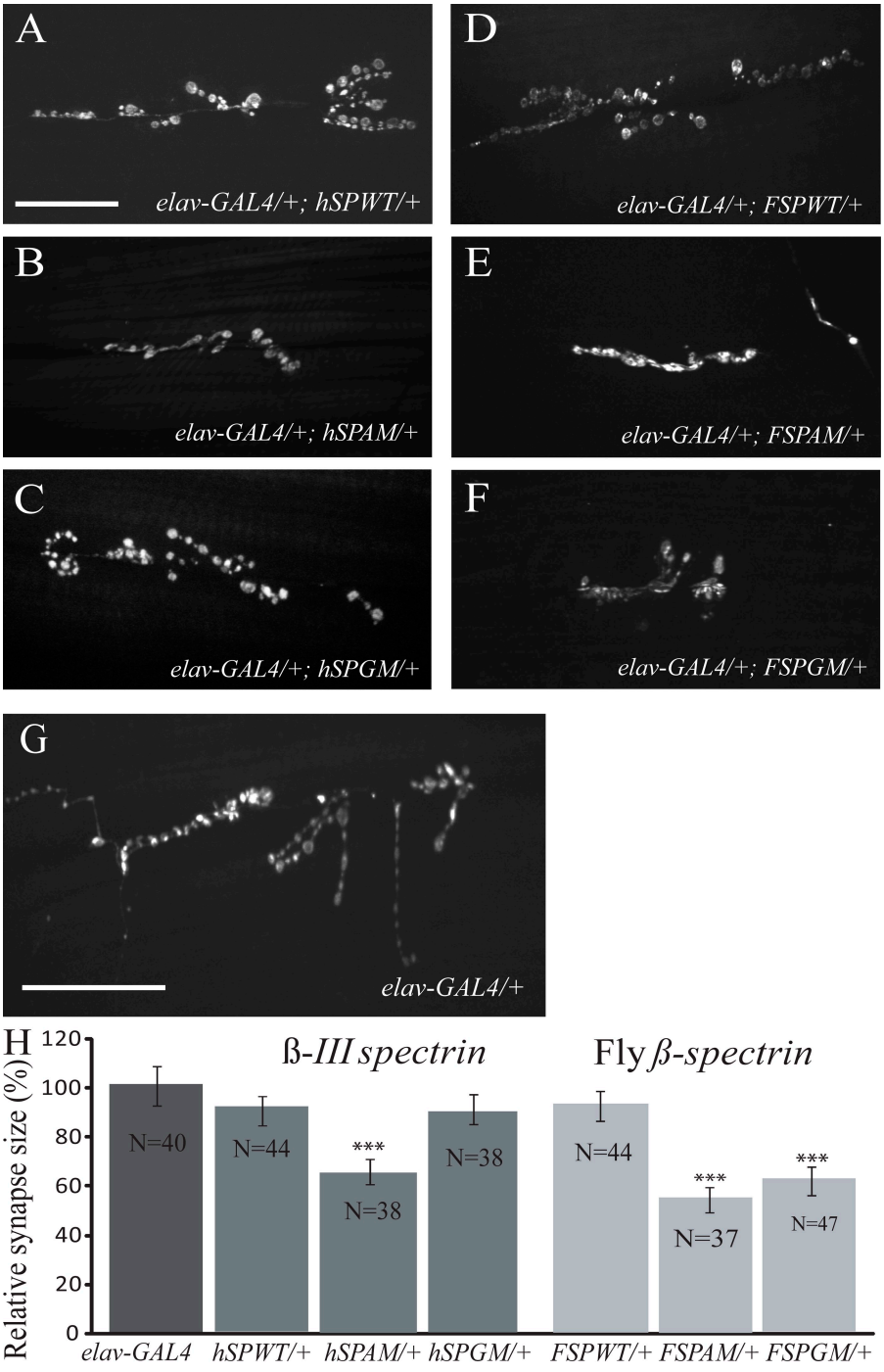

Figure 3. **Spectrin mutations affect synaptic terminal size at the NMJ.** (A–G) Confocal fluorescence images of NMJs on ventral longitudinal muscles 6/7 of larval abdominal segments 2 and 3. Larval synapses were visualized by staining with an antibody to the synaptic vesicle–associated protein CSP. Neuronal expression of the *hSPAM*, *FSPAM*, and *FSPGM* transgenes driven by *elav-GAL4* results in less NMJ expansion and fewer synaptic boutons and branches (B, E, and F) when compared with the *elav-GAL4* driver line (G). Neuronal expression of *hSPWT*, *hSPGM*, or *FSPWT* transgenes did not affect synapse size (A, C, and D). Bars, 50 µm. (H) Quantification of bouton number shows a significant reduction in synapse size (number of synaptic boutons per surface area of muscle 6/7) in larvae expressing the *hSPAM*, *FSPAM*, and *FSPGM* mutant transgenes (***, $P < 0.001$). Numbers are normalized to *elav-GAL4* in the graph. Data are mean ± SEM (error bars).

mutant [FSPAM] and German mutant [FSPGM]; Fig. S1 C). Analysis of protein expression indicates that transgenic lines for each of the genotypes in this study have comparable and approximately twofold higher levels of fly β-spectrin than the endogenous spectrin detected in the *gmr-GAL* driver line (Fig. 2 B; $P = 0.18$, $n = 4$).

Similar to the human mutant *β-III–spectrin* transgenes, the expression of the fly *β-spectrin* transgenes containing either the American (*FSPAM*) or German (*FSPGM*) mutation also produced strong degenerative eye phenotypes (Fig. 2 A, II and III). In contrast, animals overexpressing wild-type fly β-spectrin do not develop eye degeneration and only show mild ommatidial disorganization comparable to *gmr-GAL4/+* flies (*gmr-GAL4/FSPWT*; Fig. 2 A, I). These data suggest that human β-III and fly β-spectrin act in at least some of the same functional pathways when expressed in the fly and support the use of these models to study dominant or dominant-negative effects of the SCA5 mutations.

Mutant β-spectrin impairs synaptic terminal growth at the NMJ

We additionally explored the effects of the SCA5 mutations by expressing the human and fly *β-spectrin* transgenes in all neurons using the *elav-GAL4* driver, and examined synaptogenesis

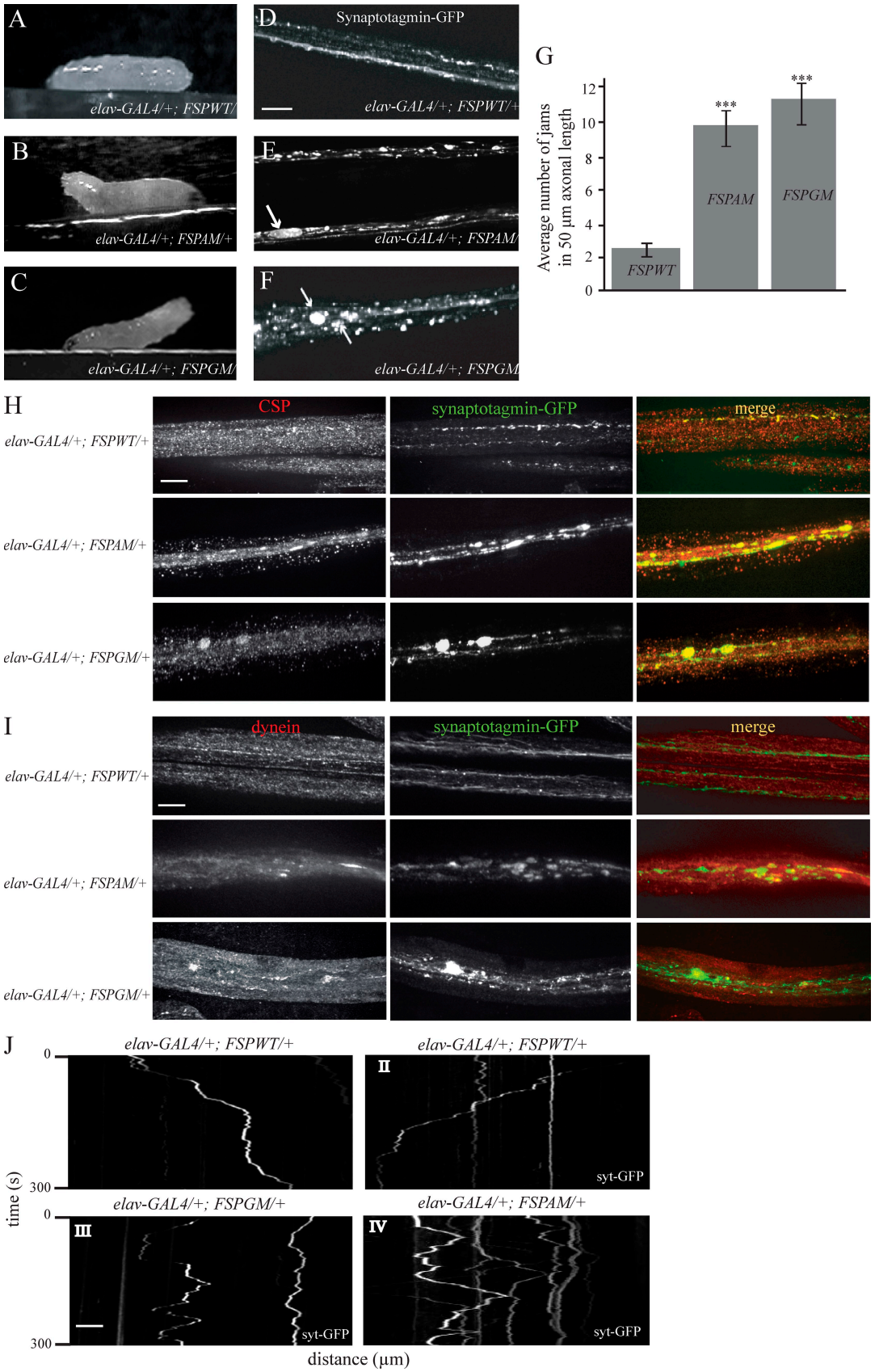

Figure 4. **Spectrin mutations disrupt the axonal transport of synaptic vesicles.** (A) Larvae overexpressing wild-type fly β-spectrin (*elav-GAL4/+; FSPWT/+*) exhibited normal posture when crawling. (B and C) Mutant larvae (*elav-GAL4/+; FSPAM/+* and *elav-GAL4/+; FSPGM/+*) developed the posterior paralysis phenotype common to axonal transport mutants in *Drosophila*. Videos of larval crawling can be seen in Videos 1–3. (D–F) The distribution of vesicular syt-GFP along larval segmental axons. Expression of the American and German mutant spectrins cause large syt-GFP accumulations (E and F) when compared

at the NMJ in third instar larvae (Fig. 3, A–G). Quantitative results are reported as relative synapse size (bouton number per muscle area; see Materials and methods) to account for differences in bouton number caused by variations in muscle size during normal growth. We observed reduced bouton number in larvae expressing mutant *hSPAM*, *FSPAM*, and *FSPGM* but not the wild-type (*hSPWT* and *FSPWT*) transgenes ($P < 0.0001$; Fig. 3). Although, under the same conditions, we did not detect differences in bouton counts in larvae expressing the *hSPGM* transgene (Fig. 3 C), this result is likely explained by the relatively low expression in this line (Fig. 1 B).

To further characterize the synaptic phenotype, we examined the organization of several proteins that are known to contribute to the spectrin-mediated development and stability of the NMJ (Pielage et al., 2006, 2008; Koch et al., 2008). In wild-type animals, the transynaptic cell adhesion molecule fasciclin II (Fas II) is organized in a honeycomb-like distribution that surrounds presynaptic active zones. In contrast, SCA5 mutant larvae have defects in the organization and morphology of synaptic boutons and in the distribution of Fas II throughout the synapse (Fig. S2) that are similar to the phenotypes described in *β-spectrin* RNAi lines. In addition, we show that the expression of mutant SCA5 transgenes does not result in synapse retraction, in contrast to results described for flies lacking β-spectrin expression at the NMJ (Pielage et al., 2005, 2006). Despite the reduction in the number of synaptic boutons observed in SCA5 mutant animals, most presynaptic terminals were found to reside in opposition to postsynaptic membranes, as indicated by costaining with the synaptic markers synaptotagmin (syt) and dics large (Dlg; Fig. S3, A–I). Our studies also show that mutant spectrin does not impair the localization of ankyrin at synaptic sites (Fig. S3, J–R) or affect microtubule organization within the axon and NMJ (Fig. S4). Taken together, these data demonstrate that the phenotypes induced by overexpression of mutant human and fly *β-spectrin* overlap, but are distinct from phenotypes previously reported by RNAi depletion of β-spectrin (Pielage et al., 2005).

Mutant β-spectrin expression impairs larval locomotion

The reduced synaptic growth observed in animals expressing mutant spectrins suggests the possibility that intracellular transport deficits contribute to the structural abnormalities at the synapse. To test this hypothesis, we examined larvae expressing the American and German SCA5 mutations for the posterior paralysis or "tail-flip" phenotype previously described for mutations that cause aberrant axonal transport (Hurd and Saxton, 1996; Martin et al., 1999; Bowman et al., 2000; Haghnia et al., 2007). Larvae expressing mutant but not wild-type fly β-spectrin in neurons exhibit the tail flip crawling phenotype due to paralysis of the posterior segments of the larval body (Fig. 4, A–C; and Videos 1–3). Although larvae expressing one copy of the human *β-III–spectrin* transgenes (*elav-GAL4/+; hSPAM/+* and *elav-GAL4/+; hSPGM/+*) did not develop similar motor defects, this likely reflects the lower levels of human protein expression compared with fly β-spectrin. Consistent with this idea, animals expressing two copies of the American mutant spectrin transgene (*elav-GAL4/+; hSPAM/hSPAM*) produce higher levels of mutant spectrin protein and exhibit the tail flip phenotype in ∼31% of the larvae (10/32 larvae; Video 4). By comparison, control animals expressing two wild-type copies of the spectrin transgene (*elav-GAL4/+; hSPWT/hSPWT*) at comparable protein levels exhibit a tail phenotype in only 5% of the larvae (2/40 larvae). In addition, if one copy of the endogenous β-spectrin gene is silenced by mutation, then a single copy of the *hSPAM* mutant transgene produces posterior paralysis in ∼32% (12/38) of larvae. In the control cross, a single copy of the wild-type human spectrin transgene (*hSPWT*) produced paralysis in <5% of the larvae (2/41). Finally, we show that RNAi depletion of the endogenous β-spectrin produces paralysis in ∼88% (29/33) of larvae, and that the introduction of two copies of the *hSPWT* transgene rescues the paralysis in ∼90% of the larvae (4/38 paralyzed). In summary, the dosage dependence of the *hSPAM* larval paralysis phenotype suggests that human and fly mutant spectrins interfere with the normal functions of wild-type β-spectrin, and that these dominant-negative effects are likely to contribute to disease.

Mutant spectrin affects both the anterograde and retrograde transport of synaptic vesicles

To determine if the larval tail paralysis and synaptogenesis phenotypes could be explained by defects in axonal transport, we analyzed the distribution of GFP-tagged synaptic vesicle membrane protein syt-GFP. In larvae expressing wild-type β-spectrin (*elav-GAL4–syt-GFP/+; FSPWT/+*), syt was evenly distributed as small puncta (Fig. 4 D). In contrast, larvae expressing mutant spectrins (*elav-GAL4–syt-GFP/+; FSPAM/+* and *elav-GAL4–syt-GFP/+; FSPGM/+*) showed an accumulation of syt-GFP–positive vesicles within axonal aggregates (Fig. 4, E and F, see arrows). Considering that segmental axons have a mean diameter of ∼0.5 µm (Rusu et al., 2007), we next quantified the number of large syt accumulations (diameter ≥ 0.7 µm), which are likely to cause axonal swellings and disrupt the normal trafficking of

with the punctuated pattern seen in axons expressing the wild-type protein (D). Large axonal swellings are indicated by arrows. (G) Quantification of the number of syt-GFP accumulations in 50 µm of axonal length. At least 15 segmental nerves were analyzed per genotype. Data represent mean ± SEM (error bars). Significant differences in the number of axonal jams between wild-type and mutants are denoted by asterisks (***, $P < 0.001$). (H) Fluorescent images of segmental nerves show the accumulation of the axonal transport cargoes syt and CSP within the axonal jams in segmental nerves from mutant but not wild-type fly β-spectrin larvae. (I) Fluorescent images of segmental axons show the accumulation of the motor protein dynein and the synaptic vesicle integral membrane protein syt in mutant but not wild-type fly β-spectrin larvae. (J) Representative kymographs showing the motion of individual syt-GFP particles in larval segmental axons as a function of time. Kymographs corresponding to larvae expressing wild-type fly β-spectrin (*elav-GAL4/+; FSPWT/+*) show fluorescent vesicles moving in one defined direction (diagonal lines), and few stationary vesicles appear as vertical lines (I and II). Kymographs from mutant spectrin larvae show stationary GFP particles, whereas the majority of those moving undergo numerous reversals in the direction of movement that appear as zigzag lines (III and IV). Bars, 10 µm.

Table I. **Analysis of syt-GFP vesicles motions in segmental nerves expressing wild-type or mutant β-spectrin driven by *elav-GAL4***

Genotype	Net velocity[a]	Number of particles	P-value
	μm/s ± SD		
elav-GAL4/+; FSPWT/+	0.75 ± 0.23	89	NA
elav-GAL4/+; FSPAM/+	0.43 ± 0.2*	88	< 0.0001
elav-GAL4/+; FSPGM/+	0.48 ± 0.15*	86	< 0.0001

Asterisks denote significant differences for mutant relative to wild-type. NA, not applicable.
[a]Net velocity was determined by adding all velocities for each tracked GFP particle over the entire time of motion. Data shown represent mean ± SD.

intracellular cargoes (Gunawardena and Goldstein, 2001). We found a significant difference (Fig. 4 G; ***, $P < 0.0001$) in the frequency of axonal jams in larvae expressing mutant *FSPAM* and *FSPGM* transgenes (Fig. 4 G) compared with wild-type controls. In addition, we show that the distributions of the synaptic vesicle protein, cysteine string protein (CSP; Fig. 4 H), as well as the dynein motor protein (Fig. 4 I), overlap with sites of syt-GFP axonal aggregates (Fig. 4, H and I).

To determine the effects of the SCA5 mutations on synaptic vesicle transport, we imaged and tracked the dynamic behavior of vesicles in live segmental axons. In flies overexpressing wild-type β-spectrin, a large number of syt-GFP–containing vesicles underwent rapid unidirectional movements. Kymograph analysis shows that this motion is characterized by long unidirectional runs (Fig. 4 J, I and II, diagonal line) interrupted by pauses and/or infrequent short reversals in the direction of vesicle transport (Fig. 4 J, I and II; and Video 5). In contrast, in segmental axons expressing either the American or German SCA5 mutations, the unidirectional bias in vesicle movement was reduced. Syt-GFP vesicles exhibited frequent reversals in the direction of transport (Fig. 4 J, zigzag line), traveling for much shorter distances in any one direction. Representative kymographs and videos that illustrate the behavior of synaptic vesicles in mutant β-spectrin axons are shown in Fig. 4 J (III and IV) and Video 6. In addition, quantitative analysis confirmed that syt-GFP vesicles moved significantly slower in mutant compared with wild-type axons (Table I). Competition by the mutant spectrins may alter the dynamics of motor attachment to vesicular cargo and/or interfere with the binding of regulatory partners that influence motor activity.

To assess whether mutant β-spectrin affects anterograde, retrograde, or both types of axonal transport, mutant spectrin and the vesicle marker neuronal synaptobrevin-GFP (n-syb-GFP) were expressed using the motor neuron–specific *D42-GAL4* driver. In control larvae (*D42-GAL4–n-syb-GFP/FSPWT*), most fluorescent particles were moving in long runs (Video 7). In contrast, animals expressing either of the mutant spectrins (*D42-GAL4–n-syb-GFP/FSPAM* and *D42-GAL4–n-syb-GFP; FSPGM*) showed numerous stationary n-syb-GFP particles, some of which were trapped within axonal swellings (Video 8). Analysis of mean velocity and run length for anterograde and retrograde movements indicate that mutant spectrin disrupts transport in both directions (Table II), and that the GFP vesicles that retained motility had slower velocities and traveled shorter distances than in controls.

Dynein–dynactin deficits genetically enhance spectrin-induced phenotypes

The rough eye and transport phenotypes caused by the mutant spectrins are similar to phenotypes previously described in dynein and dynactin mutants (McGrail et al., 1995; Martin et al., 1999; Boylan et al., 2000). If these phenotypes result from the failure of spectrin to properly engage in retrograde transport, then we would predict that dynein, and/or dynactin mutations, would enhance the mutant spectrin phenotypes. To test this hypothesis, flies carrying a hypomorphic dynein heavy chain allele ($DHC64C^{6\text{-}10}$) were crossed to flies containing a single copy of the hSPAM transgene, and progeny were scored for posterior paralysis. In contrast to single mutant animals, which do not show posterior paralysis, larvae expressing both spectrin and dynein mutations (*elav-GAL4–syt-GFP/+; hSPAM/+;* $DHC64C^{6\text{-}10}$*/+*) develop the tail flip (Fig. 5 A, III) and axonal vesicle accumulation phenotypes (Fig. 5 B, III). Additionally, double mutant larvae display significant reductions in synapse size at the NMJ compared with single mutant controls as well as *hSPWT* and *elav-GAL4* animals (Fig. 5 C; ***, $P < 0.0001$). A similar genetic interaction occurs between flies expressing the American mutation and the dominant Gl^{1} mutation in the $p150^{Glued}$ subunit of dynactin. We observed larval paralysis in 44% (22/50) of progeny carrying the American spectrin

Table II. **Analysis of transport parameters for anterograde and retrograde syb-GFP containing vesicles in wild-type and mutant segmental nerves**

Genotype	Anterograde runs					Retrograde runs				
	Velocity	P-value	Run length	P-value	*n*	Velocity	P-value	Run length	P-value	*n*
	μm ± SD		*μm/s ± SD*			*μm/s ± SD*		*μm ± SD*		
D42-GAL4; FSPWT	0.78 ± 0.13	NA	9.6 ± 2.5	NA	54	−0.72 ± 0.15	NA	9.2 ± 3.1	NA	80
D42-GAL4/FSPAM	0.5 ± 0.17*	<0.0001	6.8 ± 3.1*	<0.0001	76	−0.55 ± 0.11*	<0.0001	7.2 ± 2.5*	<0.0001	97
D42-GAL4; FSPGM	0.44 ± 0.15*	<0.0001	6.1 ± 2.7*	<0.0001	81	−0.48 ± 0.18*	<0.0001	7.4 ± 3.3*	<0.0001	135

Mean velocity and run length for both anterograde and retrograde moving particles are reduced in mutant β-spectrin larvae in comparison to wild type. Data shown represent mean ± SD. Asterisks denote statistical significant differences for mutant relative to wild type. NA, not applicable.

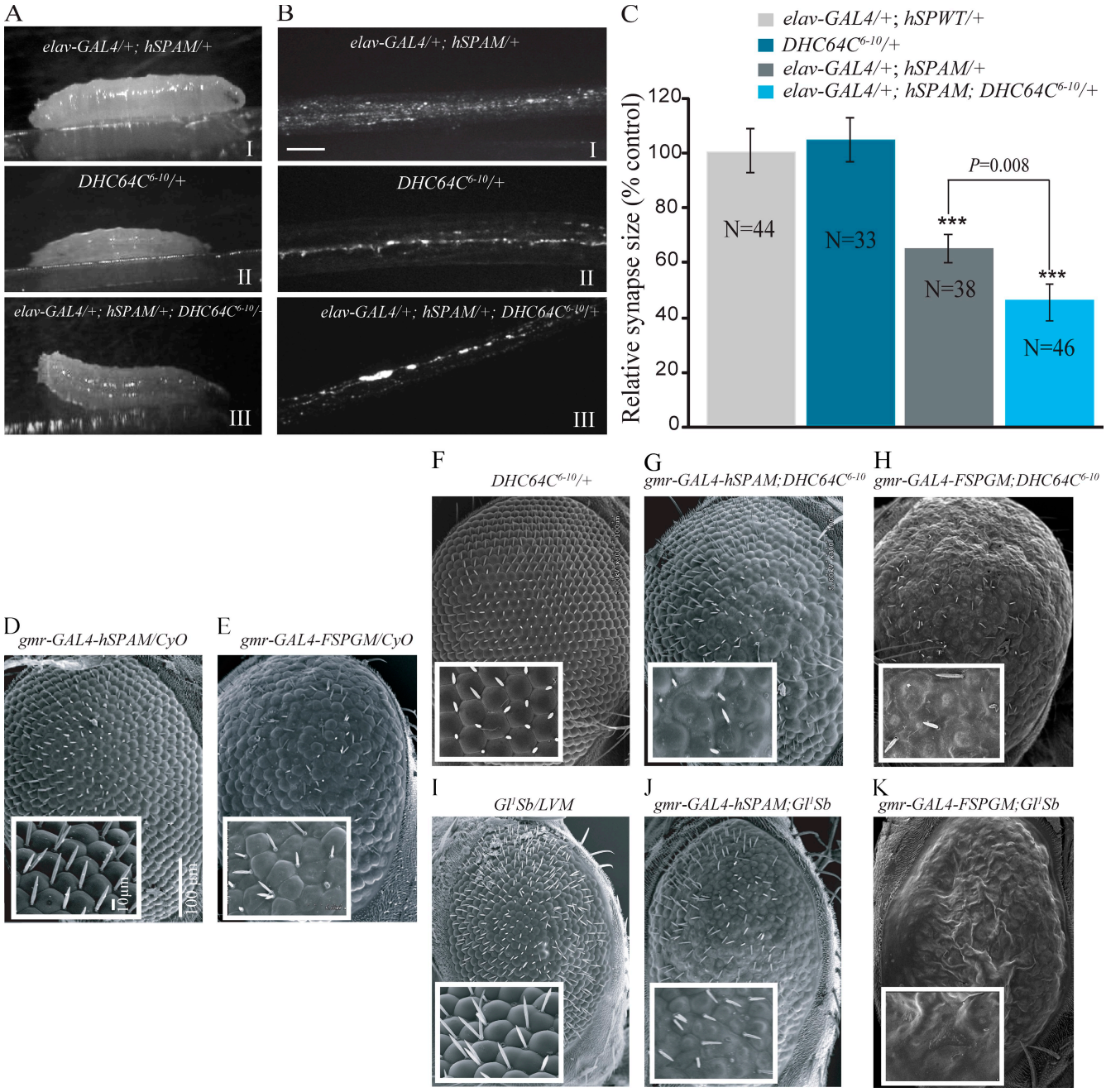

Figure 5. ***DHC64C* and *p150*^{Glued} mutant alleles enhance the dominant neurodegenerative phenotypes associated with the SCA5 mutations.** (A) Mutations in human *β-III–spectrin* interact with the cytoplasmic dynein heavy chain *DHC64C*$^{6\text{-}10}$ mutation to produce posterior paralysis. Larvae shown in A I and A II are heterozygous for the American SCA5 mutation in human *β-III–spectrin* (*elav-GAL4–syt-GFP/+, hSPAM/+*) and the *DHC64C*$^{6\text{-}10}$ mutant allele, respectively, and exhibit normal locomotion. Double heterozygous animals (*elav-GAL4–syt-GFP/+, hSPAM/+, DHC64C*$^{6\text{-}10}$*/+*) developed an abnormal crawling behavior (A III). (B) Fluorescent images show large syt-GFP accumulations within segmental nerves from double heterozygous mutant larvae (B III, *elav-GAL4–syt-GFP/+, hSPAM/+, DHC64C*$^{6\text{-}10}$*/+*). Bar, 10 µm. (C) Quantification of bouton number shows a significant reduction in synapse size (number of synaptic boutons per surface area of muscle 6/7) in animals expressing the American SCA5 mutation in human *β-III–spectrin* that are also heterozygous for the *DHC64C*$^{6\text{-}10}$ mutant allele of dynein (*elav-GAL4–syt-GFP/+, hSPAM/+, DHC64C*$^{6\text{-}10}$*/+*). Numbers are normalized and compared with the *elav-GAL4/+;hSPWT/+* control line in the graph. Data are mean ± SEM (error bars); ***, P < 0.001. (D–K) Scanning EM images of *Drosophila* eyes. Insets show higher magnification images of the ommatidial field. Recombinant lines expressing the American SCA5 mutation in *β-III–spectrin* (*gmr-GAL4-hSPAM/CyO*, 5D) or the German SCA5 mutation in fly β-spectrin (*gmr-GAL4-FSPGM/CyO*, 5E) show disorganization in the arrangement of the ommatidia and bristles of the adult eye. Note that the recombinant *gmr-GAL4-hSPAM* line showed reduced levels of transgene expression and produced a less severe eye phenotype, making it easy to distinguish changes in the phenotype. *DHC64C*$^{6\text{-}10}$*/+* flies have a wild-type eye (F) but, in combination with *gmr-GAL4-hSPAM* or *gmr-GAL4-FSPGM* mutant spectrin alleles, produce a more severe eye phenotype than either parent (G and H). Eyes expressing the dominant *Gl*^{1} mutation exhibit a rough eye phenotype, with disordered ommatidia (I). Similarly, the combination of the *Gl*^{1} dynactin mutant allele and *gmr-GAL4-hSPAM* or *gmr-GAL4-FSPGM* mutant spectrins results in a dominant enhancement of the eye degeneration. Eyes from double mutant flies are reduced in size and show a dramatic roughens of the eye surface (J and K). Bars in D also apply to F–I.

transgene in a p150^{Glued} mutant background (*elav-GAL4–syt-GFP/+; hSPAM/+; Gl^{1}/+*), whereas only 5% (5/50) of sibling progeny expressing the mutant spectrin transgene in the absence of the *Gl^{1}* (*elav-GAL4–syt-GFP/+; hSPAM/+; Tb/+*) exhibited larval paralysis. Sibling progeny (*hSPAM/+; Gl^{1}/+*) that lack the *elav-GAL4* driver showed the tail paralysis phenotype in 18% (9/50) of larvae. Additionally, the rough eye phenotypes caused by the expression of the SCA5 mutant spectrin are enhanced by dynein and dynactin mutations. This analysis was facilitated by the generation of recombinant lines that carry both the *GAL4* driver and the mutant spectrin transgenes (*gmr-GAL4-hSPAM* or *gmr-GAL4-FSPGM*) on a single chromosome (Fig. 5 D). The recombinant chromosomes, which have reduced levels of transgene expression (Fig. S5 A) develop a less severe eye phenotype (Fig. 5 D), which allowed genetically enhanced phenotypes to be more easily detected. Adult flies with one copy of the American or German mutant spectrin transgenes, which are also heterozygous for a hypomorphic mutant dynein allele, *DHC64C$^{6-10}$*, exhibit severe eye phenotypes involving disruptions of the ommatidial hexagonal packing and loss of interommatidial bristles (*gmr-GAL4-hSPAM/+; DHC64C$^{6-10}$/+* and *gmr-GAL4-FSPGM/+; DHC64C$^{6-10}$/+*; Fig. 5, G and H). In contrast, fly strains carrying only the mutant spectrin transgene or the dynein mutation exhibit only mild or wild-type eye phenotypes (Fig. 5, D–F). Similarly, the dominant *Gl^{1}* dynactin mutation, which by itself causes disorganization of the ommatidia (Fig. 5 I), genetically enhances the phenotypes of flies expressing either the American or German spectrin mutations (*gmr-GAL4-hSPAM/+; Gl^{1}/+* and *gmr-GAL4-FSPGM/+; Gl^{1}/+*; Fig. 5, J and K). We excluded the possibility that these genetic interactions simply result from alterations in spectrin expression by protein blotting (Fig. S5, B and C). The genetic interactions observed are consistent with the functional intersection of the dynein and spectrin pathways.

Discussion

We have established a series of transgenic *Drosophila* models to investigate the molecular mechanisms of spinocerebellar ataxia type 5. Toward these goals, we show that expression of the American family and German SCA5 mutations in flies causes neurodegenerative changes in the adult eye as well as motor coordination, synaptogenesis, and axonal transport deficits in *Drosophila* larvae. These phenotypes are genetically enhanced by partial loss-of-function mutations in dynein or a dominant-negative mutation in the p150^{Glued} component of dynactin. Taken together, these data demonstrate that SCA5 mutations can trigger adult-onset neurodegeneration in the fly eye and affect fundamental intracellular transport functions that are likely to play a role in this progressive neurodegenerative disease.

SCA5 mutations cause dominant dosage-dependent phenotypes

In *Drosophila*, previous work has established that the single *α-* and *β-spectrin* genes are essential (Dubreuil et al., 2000). In contrast, in humans there are four *β-spectrin* genes, and mutations in one copy of the *β-III–spectrin* gene, which is highly expressed in Purkinje cells, lead to a dominantly inherited form of ataxia (Ikeda et al., 2006). We have used ectopic expression of human β-III–spectrin and overexpression of endogenous fly β-spectrin to define the basic biological processes affected by the SCA5 mutations and to better understand the mechanisms of neurodegeneration. Our observations suggest that the human SCA5 mutations cause dominant-negative effects. Consistent with this hypothesis are data showing that the severity of the eye and larval phenotypes found in flies expressing mutant β-spectrin increases when the levels of endogenous wild-type spectrin are reduced. Our observations do not exclude the possibility that the SCA5 mutations may also cause abnormalities in protein stability and conformation that result in additional dominant gain-of-function effects. Future studies will be needed to evaluate the relative contributions of these mechanisms to the neurodegenerative Purkinje cell phenotypes seen in SCA5 patients.

The position of the German mutation in the second calponin homology domain suggests that the mutant protein disrupts the normal interactions of the wild-type protein with the actin cytoskeleton and/or the ARP1 subunit of dynactin (Holleran et al., 2001). Consistent with these data, both the German and the American mutations cause intracellular transport deficits that are similar to the phenotypes of mutant *Arp1* flies (Haghnia et al., 2007). In the case of the American family, the deletion within the third spectrin repeat may result in similar effects on dynactin pathways by disrupting protein–protein interactions that depend on the helical conformation of the spectrin repeats, and the formation of stable α-β–spectrin tetramers. The similar phenotypes found in flies expressing the SCA5 mutations in the context of either the human or fly β-spectrin proteins indicate that many of the binding partners and functional roles of spectrin are conserved between humans and flies. Indeed, antibodies specific for *Drosophila* α-spectrin can immunoprecipitate human β-III–spectrin from protein extracts (Fig. 1 L), and the human β-III–spectrin can rescue the larval tail paralysis induced after RNAi depletion of fly β-spectrin.

In *Drosophila*, the single β-spectrin gene product is the orthologue of vertebrate β-spectrins 1, 2, 3, and 4. Thus, our studies suggest that all vertebrate β-spectrins are likely capable of post-Golgi transport while potentially targeted to specific subsets of vesicular cargoes. As previously suggested (Bennett and Baines, 2001), it is unlikely that human β-III–spectrin is a general Golgi-specific protein, as axonal transport involves the trafficking of post-Golgi structures (Horton and Ehlers, 2003; Ye et al., 2007). Moreover, the expression of human β-III–spectrin is highly enriched in the cerebellum and nervous system (Sakaguchi et al., 1998), a distribution that is consistent with the localized atrophy of the cerebellar hemispheres and the neurological symptoms of SCA5 patients.

Drosophila model for SCA5

Overexpression of wild-type and mutant spectrin in *Drosophila* neurons allows us to investigate the pathways that contribute to spectrin function and regulation, and should provide insight into the molecular basis of SCA5 pathology. Although a similar approach has been exploited to study a number of other

human neurodegenerative diseases (e.g., Feany and Bender, 2000; Jinet al., 2003; Gunawardena et al., 2003; Jung and Bonini, 2007), this approach does have limitations. In contrast to the human disease, mutant spectrin is expressed in the presence of two copies of the endogenous wild-type fly *β-spectrin* gene. Although it would be interesting to compare the effects of the SCA5 mutations using a knock-in approach in which a single mutant and single wild-type *β-spectrin* allele are expressed, *Drosophila* has only a single, essential *β-spectrin* gene that is widely expressed in multiple tissues. This would limit the types of analyses that could be performed and complicate the interpretation of knock-in phenotypes. Moreover, such a knock-in fly model would not mimic the human situation in which four *β-spectrin* genes and a variety of α/β heterotetramers exhibit distinct functions and patterns of expression. Although no *Drosophila* model, including the one characterized in this study, can perfectly model a human disease, we demonstrate that the SCA5 mutant β-III–spectrins act within the normal spectrin pathway, competing with endogenous *Drosophila* β-spectrin to produce dosage-dependent phenotypes. We suggest that the phenotypes caused by overexpression of SCA5 mutant but not wild-type spectrin in our models provide insight into the molecular consequences of the mutations that are likely to be helpful in understanding the molecular mechanisms underlying the human disease.

SCA5 mutations cause synaptic deficits

The major roles of spectrin in strengthening cellular membranes and organizing ion channels, neurotransmitter receptors, cell adhesion molecules, and other components into specialized synaptic membrane domains are well established (Bloch and Morrow, 1989; Jenkins and Bennett, 2001; Lee and Discher, 2001; Komada and Soriano, 2002; Lacas-Gervais et al., 2004; Hammarlund et al., 2007; Bennett and Healy, 2008). In particular, recent work suggests that wild-type β-III–spectrin, but not SCA5 mutant spectrin, can stabilize the glutamate transporter EAAT4 at the cell membrane (Jackson et al., 2001; Ikeda et al., 2006).

Consistent with possible dominant-negative effects, expression of the SCA5 mutant proteins results in reduced numbers of synaptic boutons at synaptic termini. In *Drosophila*, spectrin function at the synapse has been extensively studied in motor neurons (Featherstone et al., 2001; Pielage et al., 2005, 2006). These studies first characterized pre- and postsynaptic spectrin localization and function during motor neuron synaptogenesis in *Drosophila*. Loss of presynaptic spectrin reportedly eliminates several essential cell adhesion molecules from synaptic sites and leads to defects in neurotransmission and the disassembly and elimination of synapses at the NMJ (Pielage et al., 2005, 2006). In addition, the RNAi depletion of presynaptic β-spectrin has been reported to disrupt microtubule organization at the terminal boutons, to generate large accumulations of synaptic vesicles with motor axons, and to reduce the accumulation of synaptic vesicles within the terminal boutons. These latter studies suggested a link between spectrin and vesicle transport either through a direct role in motor-based transport or an indirect affect on cytoskeletal organization. Although we observed similar defects in synaptic growth and trafficking in axons expressing mutant SCA5 spectrin, we also detected several distinct phenotypes. For example, synaptic retraction and loss of Fas II and Ank was reported when β-spectrin is depleted by RNAi (Pielage et al., 2005, 2006; Koch et al., 2008), but these phenotypes are not found in animals expressing SCA5 mutant spectrins. Additionally, we did not observe dramatic alterations in synaptic microtubule distribution as previously reported after depletion of presynaptic β-spectrin (Pielage et al., 2005).

To test the possible role that transport deficits play in these phenotypes, we performed a series of genetic interaction studies. We show that loss of synapses at the NMJ in SCA5 mutant flies is enhanced in animals heterozygous for dynein-heavy chain and $p150^{Glued}$ mutations. These genetic interactions suggest that spectrin, dynein, and dynactin interact in a complex that mediates synapse stabilization. Although the protein interactions that mediate synapse stability are not fully understood, one model is that synaptic components at the membrane are stabilized through spectrin and ankyrin linkages to the cytoskeleton (Pielage et al., 2006, 2008; Ayalon et al., 2008; Koch et al., 2008), and that the establishment of these connections is facilitated by dynein/dynactin recruitment of microtubules (Carminati and Stearns, 1997; Adames and Cooper, 2000; Ligon et al., 2001; Schuyler and Pellman, 2001; Dujardin and Vallee, 2002). The binding of ankyrin to the p62 subunit of dynactin, as well as the reported binding of ankyrin to microtubules, supports the hypothesis that spectrin and ankyrin may act together to stabilize the synaptic membrane through the dynactin/dynein-mediated capture of microtubules (Ayalon et al., 2008; Koch et al., 2008; Pielage et al., 2008). Consistent with this model, synapse disassembly has also been reported after disruption of dynactin function (Eaton et al., 2002).

SCA5 mutations disrupt vesicle transport

Our investigations provide the first direct in vivo visualization of spectrin's involvement in vesicle transport in neurons, in contrast to previous studies in *Drosophila* that indirectly suggested a role for β-spectrin in vesicle transport based on the accumulation of axonal cargos in fixed preparations of spectrin mutants or of motor neurons depleted of spectrins by RNAi treatment (Featherstone et al., 2001; Pielage et al., 2005, 2006). Here, we use live imaging of larval axons to directly observe the defective transport of vesicles after β-spectrin depletion by RNAi treatment, or after expression of the SCA5 mutations that specifically disrupt spectrin function. In vertebrates, the initial studies suggesting a role for spectrin in intracellular transport have been controversial. In particular, whether vertebrate β-III–spectrin is associated with Golgi vesicles has been complicated by the cross-reactivity of β-III–spectrin antisera with the related protein, nesprin (Beck, et al., 1994; Stankewich et al., 1998; Gough et al., 2003). More recent biochemical and in vitro motility studies (Muresan et al., 2001; Holleran et al., 2001) suggest a model in which two *Arp1*-binding sites on β-III–spectrin mediate the linkage between the dynein motor and cytoplasmic vesicles. In vitro imaging of protein-free liposomes or axonal vesicles from dissociated squid axoplasm shows that spectrin binding to dynactin and vesicle movement

can be inhibited by the addition of competing spectrin peptides. In our studies, we show that SCA5 mutations in β-III–spectrin disturb the retrograde and anterograde transport in axons. Velocities and run lengths of vesicles in both directions are significantly reduced, and an elevated frequency of reversals is seen. The loss of unidirectional transport may indicate a decreased affinity in the attachment of motors to vesicular cargoes and/or increased competition and switching between oppositely directed motor proteins. It will be important to understand whether compromising spectrin's function directly influences the binding of motor proteins or, alternatively, alters the binding of other factors that regulate motor activities. Although the axonal accumulations, or swellings, do not completely block the passage of moving cargoes, as synaptic vesicle proteins (e.g., syt, CSP, and syb) are transported and localized at synapses, the velocities of transport are reduced and, together with accumulation of intracellular cargos, may contribute to neurodegeneration.

Taken together, our data suggest that SCA5 is part of a growing group of diseases recently shown to involve the disruption of intracellular transport (for reviews see Chevalier-Larsen and Holzbaur, 2006; Duncan and Goldstein, 2006; De Vos et al., 2008). The fact that dynein and dynactin mutations enhance the spectrin mutant phenotypes suggests that mutant β-spectrin perturbs spectrin–dynactin interactions and affects binding of cargo to dynein (Holleran et al., 2001). Additionally, our results indicate that mutant spectrins do not only disrupt dynein-mediated retrograde transport, but also affect anterograde transport. Most likely, this reflects the interdependence between anterograde and retrograde transport that has been reported in multiple systems (Schroer et al., 1988; Brady et al., 1990; Waterman-Storer et al., 1997; Martin et al., 1999; Gross et al., 2000, 2002a,b; Pilling et al., 2006). In addition, an increasing number of biochemical and functional analyses suggest that dynactin acts as a switch to coordinate plus- and minus-end directed motor activities (Deacon et al., 2003; Gross, 2003; Haghnia et al., 2007). Our results do not exclude the possibility that the SCA5 mutations could affect kinesin-based transport (Hirokawa, 1998; De Matteis and Morrow, 2000; Takeda et al., 2000; Paik et al., 2004), even though no direct association between β-spectrin and kinesin-1 has been reported in *Drosophila*, and SCA5 phenotypes are not enhanced by kinesin mutations.

The spectrin–dynactin–dynein linkage in neurodegeneration and SCA5

Building on spectrin's ability to stabilize protein domains at the membrane, one hypothesis is that spectrin also mediates the direct association of dynein and dynactin with proteins in membrane-bound cytoplasmic vesicles (Presley et al., 1997; Holleran et al., 2001; Muresan et al., 2001). We suggest that both synapse loss and vesicle transport defects caused by the SCA5 mutations may result from disruptions in the spectrin–dynactin–dynein adapter complex that links both vesicle and synaptic membranes to microtubules. The resultant neurodegeneration likely results from defects in both activities of the spectrin–dynactin–dynein linker adapter complex. At the synaptic membrane, the spectrin adapter recruits dynactin and dynein to the plasma membrane, promoting the capture of underlying cortical microtubules and stabilization of the synaptic membrane. Phenotypes of synapse disassembly are observed when fly β-spectrin expression is reduced or dynactin is disrupted (Eaton et al., 2002; Pielage et al., 2006). The synaptic deficits caused by the human SCA5 mutations may affect similar pathways by disrupting membrane–microtubule linkages that could lead to synapse disassembly. On synaptic vesicles, the spectrin adapter links the dynactin/dynein motor complex to the membrane, providing for transport of vesicles along the axonal microtubules. In our studies, we show that SCA5 mutations inhibit the transport of vesicles both to and from the synapse in axons. Similarly, vesicle transport within dendritic processes may be disrupted by the SCA5 mutant spectrins and compromise neuronal function. Because Purkinje cells are among the largest neurons in the human central nervous system (Palay and Chan-Palay, 1974), decreased efficiency in transport of macromolecules, vesicles, and organelles, as well as the compromised stability of specialized neuronal membrane domains may underlie the profound Purkinje cell loss in SCA5 patients.

Materials and methods

Fly stocks and genetic analyses

Flies were cultured at 25°C in a 12-h light/dark cycle on standard medium. Fly stocks were obtained from the Bloomington Drosophila Stock Center unless indicated and are listed in FlyBase (http://flybase.org/).

To analyze transgene expression in the eye, homozygous virgins for each genotype were crossed to *gmr-GAL4/CyO* males. Progeny lacking curly wings were examined. Neuronal expression was driven with *elav-GAL4*. Briefly, *elav-GAL4/Y* males were mated to homozygous virgins for each genotype. Female larvae were selected for further analysis.

To generate transgenic flies expressing syt-GFP in all neurons or n-syb-GFP in motor neurons, homozygous virgins carrying wild-type or mutant spectrin transgenes were crossed to either *elav-GAL4–syt-GFP/Y* (Zhang et al., 2002) or *D42-GAL4–n-syb-GFP/TM6B, Tubby* (*Tb*) males. GFP-positive larvae were selected for analyses.

To analyze genetic interaction of spectrin mutations with $DHC64C^{6\text{-}10}$ (Gepner et al., 1996) and Gl^{1} (Harte and Kankel, 1982) mutants in the eye, standard meiotic recombination was used to generate second chromosomes carrying both the eye-specific *gmr-GAL4* driver and either the *hSPAM* or the *FSPGM* transgenes. Recombinant chromosomes were maintained over a balancer chromosome carrying the dominant maker *Curly* (*CyO*). Virgin females from *gmr-GAL4-hSPAM/CyO* or *gmr-GAL4-FSPGM/CyO* lines were mated to $Dhc64C^{6\text{-}10}$*/TM6B, D* or Gl^{1}*Sb/LVM* males. Progeny carrying the recombinant chromosomes in either the Gl^{1} or $DHC64C^{6\text{-}10}$ mutant backgrounds were identified by the absence of the dominant curly wing phenotype; the Gl^{1} mutation was identified by the bristle phenotype caused by the dominant *Sb* mutation, whereas adult flies carrying the $DHC64C^{6\text{-}10}$ mutation lacked the *curly* and *Dichaeted* wing phenotypes.

To generate larvae expressing the American SCA5 mutation in all neurons in a dynein or dynactin mutant background, homozygous virgin females (*hSPAM/hSPAM*) were crossed to *elav-GAL4-syn-GFP/Y;* $Dhc64C^{6\text{-}10}$*/TM6B, Tb* or *elav-GAL4-syn-GFP/Y;* Gl^{1}*Sb/TM6B, Tb* males. Third instar larvae that carry GFP and lack the *Tb* marker were selected for analysis.

The RNAi transgenic stock used to deplete β-spectrin in *Drosophila* larvae was provided by G. Davis (University of California, San Francisco, San Francisco, CA).

Generation of the *UASp–β-Spec* and *UAST-β-Spec* transgenic flies

To express human β-III–spectrin in *Drosophila*, full-length wild-type and mutant (American SCA5 mutation) *5′ myc-β-III–spectrin* cDNA clones (Ikeda et al., 2006) were digested with KpnI and XbaI and ligated into the *Drosophila* transformation vector *pUASp* (Rørth, 1998). For generating the German SCA5 transgene, the L253P mutation was introduced into the wild-type *5′ myc*-tagged β-III–spectrin construct (Ikeda et al., 2006) using the QuikChange II XL Site-Directed Mutagenesis kit (Agilent Technologies)

and primers German mutant forward (5′-GGGACTTACCAAGCCGCTGGATCCCGAAGAC-3′) and German mutant reverse (5′-GTCTTCGGGATCCAGCGGCTTGGTAAGTCCC-3′). The resulting product was cloned into *pUASp*. Generated *UASp* constructs containing the *human spectrin* (*hSP*) sequences are referred to here as *hSPWT* (wild-type), *hSPAM* (American mutation), and *hSPGM* (German mutation; Fig. S1 B).

The construct designed to overexpress wild-type fly β-spectrin (*FSPWT*; Fig. S1 C) was created by generating separate PCR products. Briefly, a partial cDNA clone (AT24411; Drosophila Genomics Resource Center, Indiana University, http://dgrc.cgb.indiana.edu/) containing the 5′ region of the fly *β-spectrin* mRNA was used to amplify a *KpnI–BamHI* PCR fragment using primers fly forward *KpnI* (5′-GACGGTACCGCCAAGTGAAGTTCATCC-3′) and fly reverse *BamHI* (5′-CGTACTCATCGATGTACTCGTTGCC-3′). The remained 3′ cDNA sequence was cloned using the SuperScript III One-Step RT-PCR system with Platinum Taq high fidelity (Invitrogen), total RNA from fly embryos, and the gene-specific primers fly forward *BamHI* (5′-CAGCCATGACGACGGACATTTCG-3′) and fly reverse *XbaI* (5′-AGTCTAGAGCTCTTGCTTATGGTTGCG-3′). Both PCR products were then subcloned using subsequent *KpnI–BamHI* and *BamHI–XbaI* digestions into the corresponding cloning sites of *pBluescript SK+* (Agilent Technologies) to generate the *pBluescript SK+/β-Spec* wild-type clone.

The American SCA5 mutant clone (*FSPAM*; Fig. S1 C) was generated by a PCR approach using primers fly American-Δ39 bp *BglII* forward (5′-CGTATATAAGATCTCGTTGGACAACATGGAGGAGATC-3′) and Fly American-Δ39 bp *BsrGI* reverse forward (5′-ACATCAGCTTGTACAGGCTGAGGGCGT-3′). The resulting PCR product, which deleted a 39-bp fragment in the region of homology with the deletion mutation found in the American SCA5 family (Fig. S1 B, I), was subcloned *BglII–BsrGI* into the *pBluescript SK+/β-Spec* wild-type clone. Both wild-type and the American SCA5 mutant full-length cDNAs were then cloned with *KpnI–XbaI* into the *Drosophila* transformation vector $pUAS_T$ (Brand and Perrimon, 1993).

The German SCA5 mutant clone (*FSPGM*; Fig. S1 C) was generated by introducing the L253P mutation into the *FSPWT* clone using the QuikChange II XL Site-Directed Mutagenesis kit and primers fly German mutant forward (5′-CCTGGCCAAGCCCCTTGATGCCGAG-3′) and fly German mutant reverse (5′-GTCTTCGGGATCCAGCGGCTTGGTAAGTCCC-3′).

The integrity of each construct was verified by sequencing. Transgenic flies were generated by standard *P* element–mediated germline transformation. Multiple lines of flies with independent transgene insertion were established for each genotype.

Preparation of protein extracts

Adult flies for each genotype in the study were frozen in liquid nitrogen before heads were collected and homogenized in radio immunoprecipitation assay (RIPA) lysis buffer (1× PBS, 1% Nonidet P-40, 0.5% sodium deoxycholate, and 0.1% SDS) supplemented with Complete Protease Inhibitor Cocktail Tablets (Roche). The protein supernatant was collected after centrifugation at 14,000 rpm for 30 min at 4°C and used for immunoprecipitation and Western blot analyses.

Western blot analysis

Total proteins from fly heads were separated on 4–12% gradient NuPAGE gels (Invitrogen). After electrophoresis, gels were electroblotted overnight onto nitrocellulose membranes and incubated with β-III–spectrin (1:250; Santa Cruz Biotechnology, Inc.), tubulin (1:5,000, Sigma-Aldrich), or myc (1:2,000, clone 9E10; Sigma-Aldrich) antibodies. Rabbit polyclonal anti–*Drosophila* β-spectrin antibody (a gift from D. Branton, Harvard University, Cambridge, MA) was used at a 1:5,000 dilution. Immunoreactive bands were visualized using HRP-conjugated secondary antibodies at 1:5,000 dilutions and the ECL Western blotting detection system (GE Heathcare). The ImageJ analysis software (National Institutes of Health; http://rsb.info.nih.gov/ij/) was used to quantitatively compare protein expression.

Immunoprecipitation

Protein extracts from fly heads were precleared by the addition of 100 µl of a 1:1 protein A–Sepharose suspension (GE Healthcare). After incubation on a rotator at 4°C for 2 h, this mix was centrifuged for 5 min at 5,000 rpm. Supernatant aliquots containing 400 µg of total proteins were subsequently used in immunoprecipitation experiments. In parallel, 40 µl of protein A–Sepharose beads were equilibrated in RIPA buffer supplemented with protease inhibitors and further incubated with either 10 µg of mouse anti–*Drosophila* α-spectrin antibody (clone 3A9; Developmental Studies Hybridoma Bank, University of Iowa) or 50 mg/ml of BSA during 1 h at 4°C. The antibody–bead complexes were washed free of unbound antibody and incubated with precleared protein lysates overnight at 4°C. The protein A–Sepharose beads were then collected by centrifugation for 2 min at 2,500 rpm at 4°C and washed five times with ice-cold RIPA buffer. Bound proteins were eluted with 2× SDS sample buffer and subjected to SDS-PAGE and Western blot analysis.

Scanning electron and optical microscopy of fly eyes

For scanning EM images, fly heads were dehydrated in 100% ethanol, incubated in hexamethyldisilazane (Sigma-Aldrich), dried overnight under a vacuum, and coated with gold-palladium. Images were taken with a variable pressure scanning electron microscope (S-3500N; Hitachi). For optical images, adult flies eyes were photographed with a digital camera (Nikon) attached to a stereoscope (Carl Zeiss, Inc.).

Eye histology

For histological analysis of eyes, heads from 10-d-old flies were fixed for 30 min in a 2% glutaraldehyde/2% osmium tetroxide mix, washed in PBS, fixed for an additional 3 h in 2% osmium tetroxide, and dehydrated through a graded ethanol series. Heads were further equilibrated in propylene oxide and embedded in Durcupan ACM resin (Electron Microscopy Science). Vertical semithin sections were stained with toluidine blue and photographed with a microscope (AS/LMD; Leica).

Larval motility

The behaviors of larvae were compared under a stereoscope (Carl Zeiss, Inc.). Videos of animals expressing mutant and wild-type spectrin transgenes were made using a camcorder (Nikon).

Immunohistochemistry

For immunostaining of segmental nerves, wandering third instar larvae were dissected in 1× PBS and fixed in 4% formaldehyde for 20 min as described previously (Hurd and Saxton, 1996). Larval fillets were washed three times in PBT (1× PBS and 0.1% TritonX-100) and washed for 1 h in PBT containing 1% BSA (PBT-BSA) before overnight incubation with primary antibodies at 4°C. Primary antibodies used were mouse anti-CSP (6D6, 1:250; Developmental Studies Hybridoma Bank), mouse anti-dynein heavy chain antibody (P1H4, 1:250; McGrail and Hays, 1997), and mouse anti–α-tubulin (DM1A, 1:200; Sigma-Aldrich).

To examine synaptic morphology, third instar larvae were processed and stained as described in the previous paragraph, but the ventral ganglia, brain, and segmental nerves were removed to facilitate NMJ visualization. Muscle surfaces were delimited by Alexa Fluor 488 phalloidin (Invitrogen) staining. Larval preparations were incubated overnight with primary antibodies as follows: mouse anti-futsch (22C10, 1:100), mouse anti–Fas II (1D4, 1:10), mouse anti–discs large (4F3, 1:50), mouse anti-neuroglian (BP104, 1:10; all provided by the Developmental Studies Hybridoma Bank, University of Iowa), and rabbit anti–Ank2-XL (1:1,000; a gift from H. Aberle, Westfälische Wilhelms-Universität Münster, Münster, Germany). Signals were detected with Alexa Fluor 555, Alexa Fluor 488, and Cy5-conjugated secondary antibodies (Invitrogen) used at final concentrations of 1:200 at room temperature for 2 h. Larval preparations were washed in PBT-BSA and mounted in Vectashield (Vector Laboratories).

Images of neuromuscular preparation were acquired using an inverted microscope (Eclipse TE200; Nikon) equipped with a confocal imaging system (PerkinElmer) and a digital camera (Orca ER; Hamamatsu Photonics). Synapse morphology and axonal staining were imaged using 2 × 2 binning with a 40× Plan-Apochromat (NA 1.3) and a 100× Plan-Apochromat (NA 1.4) objective, respectively, and 1-µm optical sections. Images were processed in Photoshop CS3 and Illustrator CS4 (both from Adobe).

Live imaging of GFP-tagged vesicles in larval segmental axons

Motility analyses were done on neuromuscular preparations by live confocal fluorescence microscopy. Briefly, wandering third instar larvae were dissected in HL3 buffer (Feng et al., 2004; Stewart and McLean, 2004), carefully removing gut and fat body to expose segmental nerves. GFP vesicles were imaged at 25°C with an inverted microscope (Eclipse TE200; Nikon) equipped with the confocal imaging system (PerkinElmer). Images were acquired continuously at a rate of one frame every 1 s for 300 s, with 2 × 2 binning and a 100× oil Plan-Apochromat (NA 1.4) objective, using MetaMorph software (GE Healthcare) to control a charge-coupled device camera (Orca ER).

Statistical analyses

To analyze synaptogenesis, we determined the number of synaptic boutons present per muscle area (relative synapse size). In brief, the surfaces of muscles 6 and 7 of abdominal segments 2 and 3 were delimited after Alexa Fluor 488 phalloidin staining, and total muscle surface area was determined using the "measurement" function of the MetaMorph image analysis software (MDS Analytical Technologies). The relative synapse size was calculated as the total number of synaptic boutons divided by the corresponding total muscle surface area. This relative synaptic terminal size was then averaged for each genotype and normalized as a percentage of the control numbers.

Analysis of syt-GFP accumulations within larval segmental nerves was performed as follows. Four segmental nerves were selected from the region immediately posterior to the ventral ganglion, and GFP accumulations with a diameter of at least 0.7 µm were counted along a 50-µm axonal segment, using the "analyze particle" function of the MetaMorph software. In the analyses, each genotype is represented by five larval preparations.

The movement of GFP-tagged synaptic vesicles was manually tracked with MetaMorph's "track points" function, as described previously (Mische et al., 2007). To define the direction of organelle movement, segmental nerves were oriented with the motor neurons cell bodies toward the left. Vesicle displacements toward the right were considered anterograde or plus-end runs, whereas right-to-left motions were designated retrograde or minus-end runs. Particles displaying linear movement for four consecutive frames were selected for analysis. Data from GFP particle tracking were used to calculate net velocity, mean run velocity, run length, and standard deviation for each particle using Excel software (Microsoft). Net velocity was determined when the directionality of motion could not be determined by summing all velocities displayed for one individual particle over the entire movie interval, including forward runs (positive), reverse runs (negative), and pauses. The trajectory of GFP-tagged synaptic vesicles along a portion of the segmental axon was graphed using the "kymograph" function of MetaMorph.

Statistical significance of the difference between mutant and wild-type was determined for each experiment using the Student's *t* test on unpaired data. Significance was established when $P < 0.05$.

Online supplemental material

Fig. S1 shows generation of transgenic flies expressing the SCA5 mutations. Fig. S2 shows that expression of SCA5 mutant spectrin disrupts the morphology of NMJ synapses and the organization of the cell adhesion molecule Fas II. Fig. S3 shows that expression of SCA5 mutant spectrins does not result in synapse retraction or changes in ankyrin localization at NMJ synapses. Fig. S4 shows that expression of the SCA5 mutant transgenes does not severely disrupt the organization of the microtubule cytoskeleton. Fig. S5 shows analysis of human β-III and *Drosophila* β-spectrin protein expression in lines used for genetic interaction analysis. Video 1 shows that *Drosophila* third instar larvae overexpressing wild-type fly β-spectrin in all neurons driven by *elav*-GAL4 show a normal crawling behavior. Video 2 shows that *Drosophila* third instar larva expressing the American SCA5 mutation in fly β-spectrin develops a "tail flip" phenotype during crawling. Video 3 shows that *Drosophila* third instar larva expressing the German SCA5 mutation in fly β-spectrin develop a "tail flip" phenotype during crawling. Video 4 shows that *Drosophila* third instar larva expressing two copies of the *hSPAM* transgene and higher levels of the American mutant human β-III–spectrin develop a "tail flip" phenotype during crawling. Video 5 shows motion of syt-GFP bearing synaptic vesicles in *Drosophila* segmental nerves expressing wild-type fly *β-spectrin* driven by *elav-GAL4* (*elav-GAL4–syt-GFP/+; FSPWT/+*). Video 6 shows the motion of syt-GFP–bearing synaptic vesicles in *Drosophila* segmental nerves expressing the German SCA5 mutant spectrin (*elav-GAL4–syt-GFP/+; FSPGM/+*). Video 7 shows the motion of GFP-n-syb–bearing synaptic vesicles in the motor axons of a *Drosophila* third instar larvae overexpressing wild-type fly β-spectrin (*D42-GAL4–n-syb-GFP/+; FSPWT/+*). Video 8 shows the motion of GFP-n-syb–bearing synaptic vesicles in the motor axons of a *Drosophila* third instar larvae expressing the German SCA5 mutant spectrin (*D42-GAL4–n-syb-GFP/+; FSPGM/+*). Online supplemental material is available at http://www.jcb.org/cgi/content/full/jcb.200905158/DC1.

We thank SCA5 family members for their participation, D. Branton for spectrin antibodies, H. Aberle for ankyrin antibodies, G. Davis for spectrin RNAi transgenic stocks, and H. Orr and the members of the Ranum and Hays laboratories for helpful discussions.

This work was supported by a National Institutes of Health (NIH) fellowship (1F31-NS056466) to D.N. Lorenzo; grants from the National Ataxia Foundation, the Bob Allison Ataxia Research Center, and the NIH (RO1NS056158) to L.P.W. Ranum; and an NIH award (RO1GM44757) to T.S. Hays.

Submitted: 28 May 2009
Accepted: 1 March 2010

References

Adames, N.R., and J.A. Cooper. 2000. Microtubule interactions with the cell cortex causing nuclear movements in *Saccharomyces cerevisiae*. *J. Cell Biol.* 149:863–874. doi:10.1083/jcb.149.4.863

Ayalon, G., J.Q. Davis, P.B. Scotland, and V. Bennett. 2008. An ankyrin-based mechanism for functional organization of dystrophin and dystroglycan. *Cell.* 135:1189–1200. doi:10.1016/j.cell.2008.10.018

Beck, K.A., J.A. Buchanan, V. Malhotra, and W.J. Nelson. 1994. Golgi spectrin: identification of an erythroid β-spectrin homolog associated with the Golgi complex. *J. Cell Biol.* 127:707–723. doi:10.1083/jcb.127.3.707

Bennett, V., and A.J. Baines. 2001. Spectrin and ankyrin-based pathways: metazoan inventions for integrating cells into tissues. *Physiol. Rev.* 81: 1353–1392.

Bennett, V., and J. Healy. 2008. Organizing the fluid membrane bilayer: diseases linked to spectrin and ankyrin. *Trends Mol. Med.* 14:28–36. doi:10.1016/j.molmed.2007.11.005

Bilen, J., and N.M. Bonini. 2005. *Drosophila* as a model for human neurodegenerative disease. *Annu. Rev. Genet.* 39:153–171. doi:10.1146/annurev.genet.39.110304.095804

Bloch, R.J., and J.S. Morrow. 1989. An unusual β-spectrin associated with clustered acetylcholine receptors. *J. Cell Biol.* 108:481–493. doi:10.1083/jcb.108.2.481

Bowman, A.B., A. Kamal, B.W. Ritchings, A.V. Philp, M. McGrail, J.G. Gindhart, and L.S. Goldstein. 2000. Kinesin-dependent axonal transport is mediated by the sunday driver (SYD) protein. *Cell.* 103:583–594. doi:10.1016/S0092-8674(00)00162-8

Boylan, K., M. Serr, and T.S. Hays. 2000. A molecular genetic analysis of the interaction between the cytoplasmic dynein intermediate chain and the glued (dynactin) complex. *Mol. Biol. Cell.* 11:3791–3803.

Brady, S.T., K.K. Pfister, and G.S. Bloom. 1990. A monoclonal antibody against kinesin inhibits both anterograde and retrograde fast axonal transport in squid axoplasm. *Proc. Natl. Acad. Sci. USA.* 87:1061–1065. doi: 10.1073/pnas.87.3.1061

Brand, A.H., and N. Perrimon. 1993. Targeted gene expression as a means of altering cell fates and generating dominant phenotypes. *Development.* 118:401–415.

Carminati, J.L., and T. Stearns. 1997. Microtubules orient the mitotic spindle in yeast through dynein-dependent interactions with the cell cortex. *J. Cell Biol.* 138:629–641. doi:10.1083/jcb.138.3.629

Chevalier-Larsen, E., and E.L. Holzbaur. 2006. Axonal transport and neurodegenerative disease. *Biochim. Biophys. Acta.* 1762:1094–1108.

De Matteis, M.A., and J.S. Morrow. 2000. Spectrin tethers and mesh in the biosynthetic pathway. *J. Cell Sci.* 113:2331–2343.

De Vos, K.J., A.J. Grierson, S. Ackerley, and C.C. Miller. 2008. Role of axonal transport in neurodegenerative diseases. *Annu. Rev. Neurosci.* 31:151–173. doi:10.1146/annurev.neuro.31.061307.090711

Deacon, S.W., A.S. Serpinskaya, P.S. Vaughan, M. Lopez Fanarraga, I. Vernos, K.T. Vaughan, and V.I. Gelfand. 2003. Dynactin is required for bidirectional organelle transport. *J. Cell Biol.* 160:297–301. doi: 10.1083/jcb.200210066

Dubreuil, R.R., P. Wang, S. Dahl, J. Lee, and L.S. Goldstein. 2000. *Drosophila* beta spectrin functions independently of α spectrin to polarize the Na,K ATPase in epithelial cells. *J. Cell Biol.* 149:647–656. doi:10.1083/jcb.149.3.647

Dujardin, D.L., and R.B. Vallee. 2002. Dynein at the cortex. *Curr. Opin. Cell Biol.* 14:44–49. doi:10.1016/S0955-0674(01)00292-7

Duncan, J.E., and L.S. Goldstein. 2006. The genetics of axonal transport and axonal transport disorders. *PLoS Genet.* 2:e124. doi:10.1371/journal.pgen.0020124

Eaton, B.A., R.D. Fetter, and G.W. Davis. 2002. Dynactin is necessary for synapse stabilization. *Neuron.* 34:729–741. doi:10.1016/S0896-6273(02)00721-3

Feany, M.B., and W.W. Bender. 2000. A *Drosophila* model of Parkinson's disease. *Nature.* 404:394–398. doi:10.1038/35006074

Featherstone, D.E., W.S. Davis, R.R. Dubreuil, and K. Broadie. 2001. *Drosophila* alpha- and beta-spectrin mutations disrupt presynaptic neurotransmitter release. *J. Neurosci.* 21:4215–4224.

Feng, Y., A. Ueda, and C.F. Wu. 2004. A modified minimal hemolymph-like solution, HL3.1, for physiological recordings at the neuromuscular junctions of normal and mutant *Drosophila* larvae. *J. Neurogenet.* 18:377–402. doi:10.1080/01677060490894522

Freeman, M. 1996. Reiterative use of the EGF receptor triggers differentiation of all cell types in the *Drosophila* eye. *Cell.* 87:651–660. doi:10.1016/S0092-8674(00)81385-9

Gepner, J., M.G. Li, S. Ludmann, C. Kortas, K. Boylan, S.J.P. Iyadurai, M. McGrail, and T.S. Hays. 1996. Cytoplasmic dynein function is essential in *Drosophila melanogaster*. *Genetics.* 142:865–878.

Gough, L.L., J. Fan, S. Chu, S. Winnick, and K.A. Beck. 2003. Golgi localization of Syne-1. *Mol. Biol. Cell.* 14:2410–2424. doi:10.1091/mbc.E02-07-0446

Gross, S.P. 2003. Dynactin: coordinating motors with opposite inclinations. *Curr. Biol.* 13:R320–R322. doi:10.1016/j.cub.2003.08.032

Gross, S.P., M.A. Welte, S.M. Block, and E.F. Wieschaus. 2000. Dynein-mediated cargo transport in vivo. A switch controls travel distance. *J. Cell Biol.* 148:945–956. doi:10.1083/jcb.148.5.945

Gross, S.P., M.C. Tuma, S.W. Deacon, A.S. Serpinskaya, A.R. Reilein, and V.I. Gelfand. 2002a. Interactions and regulation of molecular motors in *Xenopus melanophores*. *J. Cell Biol.* 156:855–865. doi:10.1083/jcb.200105055

Gross, S.P., M.A. Welte, S.M. Block, and E.F. Wieschaus. 2002b. Coordination of opposite-polarity microtubule motors. *J. Cell Biol.* 156:715–724. doi:10.1083/jcb.200109047

Gunawardena, S., and L.S. Goldstein. 2001. Disruption of axonal transport and neuronal viability by amyloid precursor protein mutations in *Drosophila*. *Neuron.* 32:389–401. doi:10.1016/S0896-6273(01)00496-2

Gunawardena, S., L.S. Her, R.G. Brusch, R.A. Laymon, I.R. Niesman, B. Gordesky-Gold, L. Sintasath, N.M. Bonini, and L.S. Goldstein. 2003. Disruption of axonal transport by loss of huntingtin or expression of pathogenic polyQ proteins in *Drosophila*. *Neuron.* 40:25–40. doi:10.1016/S0896-6273(03)00594-4

Haghnia, M., V. Cavalli, S.B. Shah, K. Schimmelpfeng, R. Brusch, G. Yang, C. Herrera, A. Pilling, and L.S. Goldstein. 2007. Dynactin is required for coordinated bidirectional motility, but not for dynein membrane attachment. *Mol. Biol. Cell.* 18:2081–2089. doi:10.1091/mbc.E06-08-0695

Hammarlund, M., E.M. Jorgensen, and M.J. Bastiani. 2007. Axons break in animals lacking β-spectrin. *J. Cell Biol.* 176:269–275. doi:10.1083/jcb.200611117

Harte, P.J., and D.R. Kankel. 1982. Genetic analysis of mutations at the Glued locus and interacting loci in *Drosophila melanogaster*. *Genetics.* 101:477–501.

Hirai, H., and S. Matsuda. 1999. Interaction of the C-terminal domain of delta glutamate receptor with spectrin in the dendritic spines of cultured Purkinje cells. *Neurosci. Res.* 34:281–287. doi:10.1016/S0168-0102(99)00061-9

Hirokawa, N. 1998. Kinesin and dynein superfamily proteins and the mechanism of organelle transport. *Science.* 279:519–526. doi:10.1126/science.279.5350.519

Holleran, E.A., L.A. Ligon, M. Tokito, M.C. Stankewich, J.S. Morrow, and E.L. Holzbaur. 2001. Beta III spectrin binds to the Arp1 subunit of dynactin. *J. Biol. Chem.* 276:36598–36605. doi:10.1074/jbc.M104838200

Horton, A.C., and M.D. Ehlers. 2003. Dual modes of endoplasmic reticulum-to-Golgi transport in dendrites revealed by live-cell imaging. *J. Neurosci.* 23:6188–6199.

Hurd, D.D., and W.M. Saxton. 1996. Kinesin mutations cause motor neuron disease phenotypes by disrupting fast axonal transport in *Drosophila*. *Genetics.* 144:1075–1085.

Ikeda, Y., K.A. Dick, M.R. Weatherspoon, D. Gincel, K.R. Armbrust, J.C. Dalton, G. Stevanin, A. Dürr, C. Zühlke, K. Bürk, et al. 2006. Spectrin mutations cause spinocerebellar ataxia type 5. *Nat. Genet.* 38:184–190. doi:10.1038/ng1728

Jackson, M., W. Song, M.Y. Liu, L. Jin, M. Dykes-Hoberg, C.I. Lin, W.J. Bowers, H.J. Federoff, P.C. Sternweis, and J.D. Rothstein. 2001. Modulation of the neuronal glutamate transporter EAAT4 by two interacting proteins. *Nature.* 410:89–93. doi:10.1038/35065091

Jenkins, S.M., and V. Bennett. 2001. Ankyrin-G coordinates assembly of the spectrin-based membrane skeleton, voltage-gated sodium channels, and L1 CAMs at Purkinje neuron initial segments. *J. Cell Biol.* 155:739–746. doi:10.1083/jcb.200109026

Jin, P., D.C. Zarnescu, F. Zhang, C.E. Pearson, J.C. Lucchesi, K. Moses, and S.T. Warren. 2003. RNA-mediated neurodegeneration caused by the fragile X premutation rCGG repeats in *Drosophila*. *Neuron.* 39:739–747. doi:10.1016/S0896-6273(03)00533-6

Jung, J., and N. Bonini. 2007. CREB-binding protein modulates repeat instability in a *Drosophila* model for polyQ disease. *Science.* 315:1857–1859. doi:10.1126/science.1139517

Koch, I., H. Schwarz, D. Beuchle, B. Goellner, M. Langegger, and H. Aberle. 2008. *Drosophila* ankyrin 2 is required for synaptic stability. *Neuron.* 58:210–222. doi:10.1016/j.neuron.2008.03.019

Komada, M., and P. Soriano. 2002. [β]IV-spectrin regulates sodium channel clustering through ankyrin-G at axon initial segments and nodes of Ranvier. *J. Cell Biol.* 156:337–348. doi:10.1083/jcb.200110003

Lacas-Gervais, S., J. Guo, N. Strenzke, E. Scarfone, M. Kolpe, M. Jahkel, P. De Camilli, T. Moser, M.N. Rasband, and M. Solimena. 2004. βIVΣ1 spectrin stabilizes the nodes of Ranvier and axon initial segments. *J. Cell Biol.* 166:983–990. doi:10.1083/jcb.200408007

Lee, J.C., and D.E. Discher. 2001. Deformation-enhanced fluctuations in the red cell skeleton with theoretical relations to elasticity, connectivity, and spectrin unfolding. *Biophys. J.* 81:3178–3192. doi:10.1016/S0006-3495(01)75954-1

Ligon, L.A., S. Karki, M. Tokito, and E.L. Holzbaur. 2001. Dynein binds to beta-catenin and may tether microtubules at adherens junctions. *Nat. Cell Biol.* 3:913–917. doi:10.1038/ncb1001-913

Liquori, C.L., L.W. Schutt, H.B. Clark, J.W. Day, and L.P. Ranum. 2002. Spinocerebellar ataxia type 5 (SCA5). *In* The Cerebellum and its Disorders, M.U. Manto and M. Pandolfo, editors. Cambridge University Press, Cambridge. 445–450.

Martin, M.A., S.J. Iyadurai, A. Gassman, J.G. Gindhart Jr., T.S. Hays, and W.M. Saxton. 1999. Cytoplasmic dynein, the dynactin complex, and kinesin are interdependent and essential for fast axonal transport. *Mol. Biol. Cell.* 10:3717–3728.

McGrail, M., and T.S. Hays. 1997. The microtubule motor cytoplasmic dynein is required for spindle orientation during germline cell divisions and oocyte differentiation in *Drosophila*. *Development.* 124:2409–2419.

McGrail, M., J. Gepner, A. Silvanovich, S. Ludmann, M. Serr, and T.S. Hays. 1995. Regulation of cytoplasmic dynein function in vivo by the *Drosophila* Glued complex. *J. Cell Biol.* 131:411–425. doi:10.1083/jcb.131.2.411

Mische, S., M. Li, M. Serr, and T.S. Hays. 2007. Direct observation of regulated ribonucleoprotein transport across the nurse cell/oocyte boundary. *Mol. Biol. Cell.* 18:2254–2263. doi:10.1091/mbc.E06-10-0959

Muresan, V., M.C. Stankewich, W. Steffen, J.S. Morrow, E.L. Holzbaur, and B.J. Schnapp. 2001. Dynactin-dependent, dynein-driven vesicle transport in the absence of membrane proteins: a role for spectrin and acidic phospholipids. *Mol. Cell.* 7:173–183. doi:10.1016/S1097-2765(01)00165-4

Paik, J.E., N. Kim, S.S. Yea, W.H. Jang, J.Y. Chung, S.K. Lee, Y.H. Park, J. Han, and D.H. Seog. 2004. Kinesin superfamily KIF5 proteins bind to beta-III spectrin. *Korean J. Physiol. Pharmacol.* 8:167–172.

Palay, S., and V. Chan-Palay. 1974. Cerebellar Cortex: Cytology and Organization. Springer, Berlin. 348 pp.

Pielage, J., R.D. Fetter, and G.W. Davis. 2005. Presynaptic spectrin is essential for synapse stabilization. *Curr. Biol.* 15:918–928. doi:10.1016/j.cub.2005.04.030

Pielage, J., R.D. Fetter, and G.W. Davis. 2006. A postsynaptic spectrin scaffold defines active zone size, spacing, and efficacy at the *Drosophila* neuromuscular junction. *J. Cell Biol.* 175:491–503. doi:10.1083/jcb.200607036

Pielage, J., L. Cheng, R.D. Fetter, P.M. Carlton, J.W. Sedat, and G.W. Davis. 2008. A presynaptic giant ankyrin stabilizes the NMJ through regulation of presynaptic microtubules and transsynaptic cell adhesion. *Neuron.* 58:195–209. doi:10.1016/j.neuron.2008.02.017

Pilling, A.D., D. Horiuchi, C.M. Lively, and W.M. Saxton. 2006. Kinesin-1 and dynein are the primary motors for fast transport of mitochondria in *Drosophila* motor axons. *Mol. Biol. Cell.* 17:2057–2068. doi:10.1091/mbc.E05-06-0526

Presley, J.F., N.B. Cole, T.A. Schroer, K. Hirschberg, K.J. Zaal, and J. Lippincott-Schwartz. 1997. ER-to-Golgi transport visualized in living cells. *Nature.* 389:81–85. doi:10.1038/38891

Rørth, P. 1998. Gal4 in the *Drosophila* female germline. *Mech. Dev.* 78:113–118. doi:10.1016/S0925-4773(98)00157-9

Rusu, P., A. Jansen, P. Soba, J. Kirsch, A. Löwer, G. Merdes, Y.H. Kuan, A. Jung, K. Beyreuther, O. Kjaerulff, and S. Kins. 2007. Axonal accumulation of synaptic markers in APP transgenic *Drosophila* depends on the NPTY motif and is paralleled by defects in synaptic plasticity. *Eur. J. Neurosci.* 25:1079–1086. doi:10.1111/j.1460-9568.2007.05341.x

Sakaguchi, G., S. Orita, A. Naito, M. Maeda, H. Igarashi, T. Sasaki, and Y. Takai. 1998. A novel brain-specific isoform of beta spectrin: isolation and its interaction with Munc13. *Biochem. Biophys. Res. Commun.* 248:846–851. doi:10.1006/bbrc.1998.9067

Schroer, T.A., B.J. Schnapp, T.S. Reese, and M.P. Sheetz. 1988. The role of kinesin and other soluble factors in organelle movement along microtubules. *J. Cell Biol.* 107:1785–1792. doi:10.1083/jcb.107.5.1785

Schuyler, S.C., and D. Pellman. 2001. Search, capture and signal: games microtubules and centrosomes play. *J. Cell Sci.* 114:247–255.

Stankewich, M.C., W.T. Tse, L.L. Peters, Y. Ch'ng, K.M. John, P.R. Stabach, P. Devarajan, J.S. Morrow, and S.E. Lux. 1998. A widely expressed betaIII spectrin associated with Golgi and cytoplasmic vesicles. *Proc. Natl. Acad. Sci. USA.* 95:14158–14163. doi:10.1073/pnas.95.24.14158

Stewart, B.A., and J.R. McLean. 2004. Population density regulates *Drosophila* synaptic morphology in a Fasciclin-II-dependent manner. *J. Neurobiol.* 61:392–399.

Takeda, S., H. Yamazaki, D.H. Seog, Y. Kanai, S. Terada, and N. Hirokawa. 2000. Kinesin superfamily protein 3 (KIF3) motor transports fodrin-associating vesicles important for neurite building. *J. Cell Biol.* 148:1255–1265. doi:10.1083/jcb.148.6.1255

Waterman-Storer, C.M., S.B. Karki, S.A. Kuznetsov, J.S. Tabb, D.G. Weiss, G.M. Langford, and E.L. Holzbaur. 1997. The interaction between cytoplasmic dynein and dynactin is required for fast axonal transport. *Proc. Natl. Acad. Sci. USA.* 94:12180–12185. doi:10.1073/pnas.94.22.12180

Ye, B., Y. Zhang, W. Song, S.H. Younger, L.Y. Jan, and Y.N. Jan. 2007. Growing dendrites and axons differ in their reliance on the secretory pathway. *Cell.* 130:717–729. doi:10.1016/j.cell.2007.06.032

Zhang, Y.Q., C.K. Rodesch, and K. Broadie. 2002. Living synaptic vesicle marker: synaptotagmin-GFP. *Genesis.* 34:142–145. doi:10.1002/gene.10144